Space Science Reviews (2023) 219:33
https://doi.org/10.1007/s11214-023-00976-w

On the Physical Nature of the so-Called Prominence Tornadoes

Stanislav Gunár[1] · Nicolas Labrosse[2] · Manuel Luna[3] · Brigitte Schmieder[4,5,2] · Petr Heinzel[1,6] · Therese A. Kucera[7] · Peter J. Levens[2] · Arturo López Ariste[8] · Duncan H. Mackay[9] · Maciej Zapiór[1]

Received: 23 February 2023 / Accepted: 29 April 2023

Abstract
The term 'tornado' has been used in recent years to describe several solar phenomena, from large-scale eruptive prominences to small-scale photospheric vortices. It has also been applied to the generally stable quiescent prominences, sparking a renewed interest in what historically was called 'prominence tornadoes'. This paper carries out an in-depth review of the physical nature of 'prominence tornadoes', where their name subconsciously makes us think of violent rotational dynamics. However, after careful consideration and analysis of the published observational data and theoretical models, we conclude that 'prominence tornadoes' do not differ in any substantial way from other stable solar prominences. There is simply no unequivocal observational evidence of sustained and coherent rotational movements in quiescent prominences that would justify a distinct category of prominences sharing the name with the well-known atmospheric phenomenon. The visual impression of the column-like silhouettes, the perceived helical motions, or the suggestive Doppler-shift patterns all have a simpler, more likely explanation. They are a consequence of projection effects combined with the presence of oscillations and/or counter-streaming flows. 'Prominence tornadoes' are thus just manifestations of the complex nature of solar prominences when observed in specific projections. These coincidental viewing angles, together with the presence of fine-structure dynamics and simple yet profoundly distorting projection effects, may sometimes play havoc with our intuitive understanding of perceived shapes and motions, leading to the incorrect analogy with atmospheric tornadoes.

Keywords Solar prominences · Observational diagnostics · Spectroscopy · Modelling

1 Introduction

Solar prominences are three-dimensional, dynamic and highly structured solar phenomena that we can observe only in two-dimensional projections either above the solar limb or against the solar disk. When we observe prominences as dark, absorbing structures against the bright solar disk, we refer to them as filaments. We know that the plasma of prominences is significantly cooler and denser than the surrounding coronal environment. This is possible due to the presence of the prominence magnetic field that supports the dense prominence material against gravity and insulates the cool plasma from the much hotter corona.

Extended author information available on the last page of the article

However, the real nature of prominences is more complex than such a general description can convey. First, the plasma of prominences is multi-thermal and multi-baric, ranging from the coolest (<10,000 K), high-density cores of prominence fine structures to high coronal temperatures and low pressures, forming a complex transition region. A complete understanding of this so-called Prominence-Corona Transition Region (PCTR) is still elusive and the detailed distribution of the prominence plasma at different temperature and pressure intervals inside PCTR is largely unknown.

Second, the configurations of the prominence magnetic field are generally understood to contain large regions where the topology of the field is horizontal or dipped. The dense and cool prominence plasma located in such magnetic dips can remain in the corona relatively unperturbed for long periods of time. Such a picture seems to be necessary if we want to explain the long lifetimes of quiescent prominences that may reach weeks or even a few months. Other scenarios aiming to explain long lifetimes of prominences require ever-present dynamics continually resupplying the prominence mass and/or kinetically supporting the prominence material against gravity.

The third factor complicating our understanding of prominences is their dynamics. Even the long-lived quiescent prominences are composed of numerous fine structures that seem to continually appear and disappear on timescales as short as a few minutes.

This conundrum is not helped by the actual nature of our observational techniques. The imaging, spectral or spectro-polarimetric observations we employ are obtained at various wavelengths ranging from radio to the extreme ultraviolet. Thanks to this wide spectral range, we can sample different layers of the prominence plasma having different thermodynamic properties but also widely varying optical thickness. Such a sampling of different constituents of the multi-thermal and multi-baric prominence plasma can often lead to dramatically different appearance of the same prominences in observations obtained at different wavelengths.

Yet another factor clouding our intuitive judgement of the prominence nature are the projection effects that are always present when inherently 3D structures strongly affected by spherical geometry are observed in projections onto a 2D plane. Indeed, the dimensions of prominences are such that the curvature of the solar sphere plays an important role in the aspect they show to the observer. For example, a simple case of a plasma moving above the solar surface along a horizontal trajectory with a length of 200 Mm (analogous to a typical length of quiescent prominences) which crosses the limb at a near-perpendicular angle will to an observer appear to move vertically, raising in one end and falling in the other. This is a familiar situation to any prominence observer: what looks like an arch over the limb is actually a straight and horizontal filament with respect to the local direction of gravity. This way, horizontal plasma motions within prominences are easily converted into apparent vertical movements just by perspective.

Clearly, solar prominences are complex phenomena coupling together multi-thermal, multi-baric, and partially ionised plasma, magnetic field, and various forms of dynamics. More information on the properties of the prominence plasma and the structure of their magnetic field can be found in reviews of Labrosse et al. (2010), Mackay et al. (2010), in the proceedings of the IAU 300 Symposium edited by Schmieder et al. (2014a) or in the book Solar Prominences edited by Vial and Engvold (2015). Prominence observations were reviewed by Parenti (2014) and modeling by Gibson (2018).

In the present paper, we focus on the physical nature of the type of prominences called prominence tornadoes. These resemble vertical structures that would be generally identified as prominence feet or barbs if it were not for the fact that they appear to show rotational motions around the more or less vertical axis in movies obtained by several instruments

in several spectral domains. This apparent rotation has been corroborated by several measurements of Doppler shifts showing the characteristic change of sign of the line-of-sight velocity at both sides of the axis of rotation. As presented, there might be little doubt that what one sees is indeed a vertical column of plasma rotating around its axis, justifying the name given to it by its analogy with the terrestrial atmospheric phenomenon. However, this analogy with tornadoes is only morphological and does not extend to the existence of analogous mechanisms causing atmospheric tornadoes nor to the actual properties of tornadoes on Earth.

Nevertheless, the analogy with a tornado that continually rotates around its vertical axis strongly collides with the usual paradigm of the magnetic structure of solar prominences. The vivid and sometimes chaotic movements seen in both cool and hot plasma in and around some prominences are in contrast with the apparently stable and long-lived horizontal magnetic field topology measured with state-of-the-art techniques in that very same plasma. As we mentioned earlier, the cool plasma of prominences is thought to be located in the dips of the prominence magnetic field with the topology of a flux rope or a sheared arcade – see Mackay et al. (2010) or Gibson (2018) for an extensive discussion of the configurations of the prominence magnetic field. Such dips are actually shallow compared to the length of the magnetic structure, having depths of a few hundred to a few thousand kilometres compared to total lengths of tens to hundreds of Mm. Within such predominantly horizontal magnetic field configurations, the vertical structures of prominences (including prominence feet, or barbs) are created as pile-ups of horizontal dips (see, e.g., Aulanier and Démoulin 1998; Dudík et al. 2008; Gunár and Mackay 2015a,b). If the prominence plasma sits in horizontal field lines, what is turning in the prominence tornado? Is the cool plasma suddenly crossing field lines in spite of the low value of the plasma β parameter, or is it rather just following helical magnetic field lines? Are we seeing signatures of mostly vertical magnetic field lines describing such an helix before joining the horizontal structure of the flux rope or of the sheared arcade supporting the main body of the prominence? But if such is the case we should expect the coiling magnetic field lines to raise the magnetic tension in the prominence magnetic field configurations rendering them unstable. However no prominence seems to have been destabilised by the presence of even several simultaneous 'prominence tornadoes' at its feet. Moreover, how is the dense plasma of prominences supported against gravity in such helical magnetic field configurations with a strong vertical component? Seeing such questions, it should come as no surprise that the observations suggesting the existence of prominence tornadoes seemingly rotating around a vertical axis appear to wreak havoc on decades-long measurements, theory and modelling of prominence magnetic fields and their plasma.

In the present paper, we provide a comprehensive review of the current state of understanding of 'prominence tornadoes'. This work and its conclusions are based on our wide-ranging discussions facilitated by the International Space Science Institute in Bern which funded International Team 374.[1] In the paper, we review and summarise historical and recent observations of solar prominences named 'prominence tornadoes' and analyse their findings. We also provide an in-depth discussion of the results of the latest theoretical works that are associated with rotation-like dynamics of prominences and their fine structures. This allows us to illuminate the physical nature of 'prominence tornadoes', phenomena that attracted significant attention within the last decade. Indeed, the term 'prominence tornadoes' has recently been used to describe features of both large-scale eruptive prominences and generally stable quiescent prominences. The latter are the focus of this work. Even in the

[1] http://www.issibern.ch/teams/prominenceparadox/

case of quiescent prominences, the term 'tornado' and the associated notions of rotational dynamics are used for two distinct observed configurations – vertical column (or funnel) like structures and horizontal structures clearly showing helical features. However, as this paper makes clear, these two types of 'prominence tornadoes' do not show many similarities, apart from the fact that the perceived rotational motions can be more plausibly explained by the projection effects and the presence of oscillations and/or counter-streaming flows. The detailed examination of the current observational and theoretical evidence thus leads us to conclude that there is no sustained and coherent rotation in the 'prominence tornadoes'. These do not differ from other prominences and are in fact just manifestations of the same phenomena coincidentally observed in specific projections.

2 Photospheric and Chromospheric Swirls

Apart from prominences, the terms 'tornado', 'giant tornado', or 'magnetic tornado' have also been used to describe features with swirling, rotational characteristics that are observed in the lower solar atmosphere. These 'swirls' – discovered by Bonet et al. (2008) and comprehensively reviewed by Tziotziou et al. (2023) – are not associated with prominences and thus are not the focus of this paper. However, it is important to emphasize here the clear distinction between the small-scale photospheric and chromospheric vortex flows observed from above on the solar disk and much more extended prominences observed from the side above the solar limb. The vortex flows identified in the lower solar atmosphere in high-resolution observations and numerical simulations were classified in Wedemeyer et al. (2013b). These authors note, that the observable signatures of these vortices – dubbed 'magnetic tornadoes' – "can be very subtle and difficult to detect given the dynamic changes in the solar chromosphere". These 'tornadoes', which are akin to the 'tornado' observed by Pike and Mason (1998), are not related to any filament or prominence structures.

Wedemeyer-Böhm et al. (2012) reported on "magnetic tornadoes" which appeared on disc as apparent swirling motions in the photosphere and chromosphere. These convectively driven vortex flows appear to be abundant in the photosphere and were shown by Wedemeyer-Böhm et al. (2012) to also extend into the chromosphere. The chromospheric swirls are observed as "rotating rings or ring fragments" with typical diameters of the order of 1,500 km and lifetimes of about 10-15 minutes. The heights of these structures (sometimes called 'super tornadoes') are difficult to estimate from observations, however they were modelled up to a few thousands km above photosphere. These dimensions show that the photospheric or chromospheric swirls are rather compact in the context of prominences. Their observed sizes are at the level of the dimensions of prominence and filament fine structures (see, e.g., Lin et al. 2008). The observed lifetimes of these vortex flows are also much shorter than the lifetimes of prominences (but might be comparable with the lifetimes of prominence fine structures). The LOS velocities observed in the chromospheric swirls are of the order of 4 km s^{-1} (Wedemeyer-Böhm et al. 2012). However these are upward velocities that are parallel to the (vertical) rotational axis. That is in contrast with the LOS velocities observed in prominences above the solar limb, which represent horizontal motions perpendicular to the supposed rotational axis. The horizontal velocities modelled in the chromospheric swirls reach up to about 10 km s^{-1} (see, e.g., Wedemeyer and Steiner 2014).

A chromospheric vortex ('tornado') with similar characteristics as those of Wedemeyer-Böhm et al. (2012) was reported also by, for example, Tziotziou et al. (2018). Moreover,

even smaller vortex flows spanning the photospheric and chromospheric layers were identified in simulations by Yadav et al. (2020, 2021) and Silva et al. (2020, 2021). These vortices with cross-sections as small as 100 km are at the limit of the resolution of the used simulations. Indeed, the actual spatial resolution of the simulations or observations may play a crucial role in the identification of these rotational features. With the increasingly better resolution, individual swirls might be detected at different places suggesting that the true dimensions of these vortex flows could be at the level of the convectively driven turbulence scale. Even if that would not be the case, the currently observed photospheric and chromospheric 'tornadoes' represent much more compact phenomena than the prominence barbs or legs discussed in the present paper.

3 Historical Observations of Prominence Tornadoes

In this section, we present an overview of historical aspects of 'prominence tornado' observations. This overview is an adaptation of an extensive discussion of early observations of 'prominence tornadoes' published in the PhD Thesis of Levens (2018).[2]

Prominences with a spiral structure, somewhat resembling a terrestrial tornado, were first shown by Secchi (1877) under the term 'Flammes'. Secchi describes that the 'flammes' have a spiralling motion, which is only visible in projection when they are viewed above the solar limb. This description is likely to be one of the first reports of spiralling motions in a prominence. The term 'tornado' was first used in the morphological description of solar prominences by Pettit (1925). These early identifications of prominences with tornado-like features were done in the bright Hα emission line. Pettit described them as being "very small, generally 10″ or 15″ in diameter and 1″ or 2″ high". He also noted that they "appear like closely twisted rope or a fine screw", and at the time thirty cases had been recorded in photographic observations from Yerkes Observatory. In the top panels of Fig. 1, we show an example from the 'tornado prominence' class (Class 4 Pettit 1932). These observations obtained on 5 July 1928 show photographs taken in approximately five-minute intervals. With the benefit of hindsight based on the current knowledge, we could nowadays describe

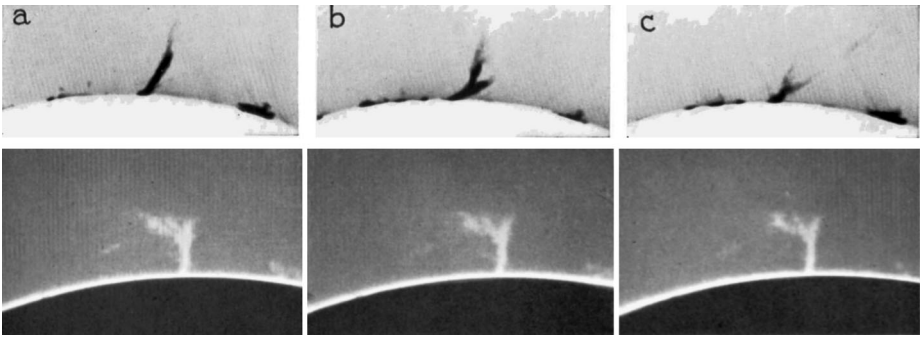

Fig. 1 Examples of the 'tornado' class of prominences (Class 4), as defined by Pettit (1932), observed in Hα. *Top:* Observations from 5 July 1928 from Pettit (1932). These images are in negative intensity. Panels *a*, *b*, and *c* were photographed approximately 5 minutes apart. Bottom: Observations from 19 September 1941 from Pettit (1943). Photographs were taken at 15 minute intervals

[2] https://theses.gla.ac.uk/8684/7/2018LevensPhd.pdf

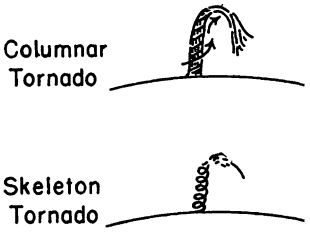

Fig. 2 Sketches of the two tornado sub-classes defined by Pettit (extracted from Fig. 1 of Pettit 1943). The top sketch is of a 'columnar tornado', and the bottom is of a 'skeleton tornado'

this prominence as highly active, perhaps at the onset of an eruption. The bottom panels of Fig. 1 show a later example from 19 September 1941 (Pettit 1943), with 15 minutes between each photograph. Since there seems to be very little change in the large-scale structure of this prominence, we are probably looking at a quiescent prominence. The resemblance to a terrestrial tornado is not due to any apparent rotational motions but in the silhouette of a dense vertical column with a wide, funnel-like top. This shape might be loosely associated with the dark clouds typically appearing above atmospheric tornadoes but is in fact a usual feature of quiescent prominences. Spiralling features were noted a number of years earlier by the same author (Pettit 1919) with regards to an erupting prominence that "began to show a spiral structure, as if the whole body were twisted into a giant spring" – behaviour that continued until the prominence erupted entirely. This earlier report of a twisted structure appears different to the 'tornado' classification, which was used only to describe vertical columns of quiescent prominences.

The tornado classification was further refined in Pettit (1943), where two sub-classes were identified – 'columnar tornadoes' and 'skeleton tornadoes' (Fig. 2). Columnar tornadoes were described as being dense, twisted columns that resembled "closely wound springs or fine-threaded screws". Skeleton tornadoes, on the other hand, were much less tightly wound. Pettit described them as "individual twisting streamers, which give them the appearance of a crossed latticework". In both cases, Pettit believed that they were rotating columns, calling them a 'vortex' and that they would dissipate if the rotational velocity became too large. For example, using a series of photographs Pettit (1941) estimated that one tornado prominence had a rotational velocity of 54 km s^{-1}. Pettit (1946) was also able to observe the spectrum of a group of tornado prominences using a spectroheliograph and measure the Doppler shift of the Hα line. From that study, Pettit found that each prominence column had a redshift down one side, and a blueshift down the other, indicating rotational motion. He determined that each of the tornadoes was rotating with velocities of 2–4 km s^{-1}, much smaller than the 54 km s^{-1} he had previously estimated from images alone. Pettit (1946) acknowledged this difference and noted that the earlier prominence was much more active than the latter ones, eventually erupting, which gave the reason why the calculated velocities were much higher.

Other observers reported on tornado-class prominences in the 1940s, with Richardson (1940) noting a "tornado prominence of record height" of impressive 240 Mm ($\sim 0.3 R_\odot$, clearly indicating a later stage of a prominence eruption), and Nicholson (1944) also reporting an erupting tornado prominence. The observations of tornado prominences up to 1950 were well summarised in Pettit (1950), where he concluded that: 1) Tornado prominences had been observed using imaging and spectroscopic techniques; 2) Some tornado prominences show signs of activity, with plasma streaming from their tops back to the chromosphere; 3) They are anchored at the solar surface, unmoving in solar latitude; 4) They rotate around a central axis, with rotation observed both spectroscopically and using image series; 5) They disappear when their rotational velocity becomes too large or when they erupt.

After the works of Pettit, there were very few mentions of tornado prominences for a long time. Rotational motions in filaments were reported by Öhman (1969), but these were of a different nature than those described by Pettit. Rompolt (1975) discussed spectral characteristics of possible rotational motions in different types of solar structures, such as filaments, surges, flares, spicules, and prominence knots. An observation of an eruptive prominence in 1990 at the Yunnan Observatory in China prompted some discussion of tornado-like motions (Zhong and Li 1994; Li and Zhong 1997), but this erupting prominence was not the same as the more quiescent tornado prominences that were discussed earlier. The term 'tornado' was also used by Pike and Mason (1998) to describe rotational motions in so-called macrospicules but these do not bear any relationship to a prominence.

4 Contemporary Observations of Prominence Tornadoes

With the launch of the Solar Dynamics Observatory (SDO; Pesnell et al. 2012) and its high-resolution Atmospheric Imaging Assembly (AIA; Lemen et al. 2012) in 2010, authors became interested in tornadoes in relation to prominences again. In 2012 three letters were published that reported tornado-like motions in prominences (Li et al. 2012; Su et al. 2012; Orozco Suárez et al. 2012).

Li et al. (2012) reported a helical structure in the top part of a prominence observed by SDO/AIA, which we show in Fig. 3. The prominence appears bright in the AIA coronal wavebands (171, 193 and 211 Å), strongly indicating a heating of the observed plasma. The dark cavity surrounding the prominence suggests that we are seeing the prominence magnetic field configuration with the line of sight parallel to the axis of the flux rope (see, e.g., Gibson 2015). The helical configuration of the observed prominence fine structure is also consistent with the idea of a view along the flux rope axis. This event was also studied by Panesar et al. (2013), who noted that the activity and the apparent heating in this prominence could have been caused by a nearby flaring region. The term 'prominence tornado' used in these papers refers to different structures than those classified by Pettit, however. The axis of its cyclonic component is horizontal (i.e. parallel to the solar surface) as opposed to a vertical. This cyclonic dynamics is well visible for example in the movie processed by

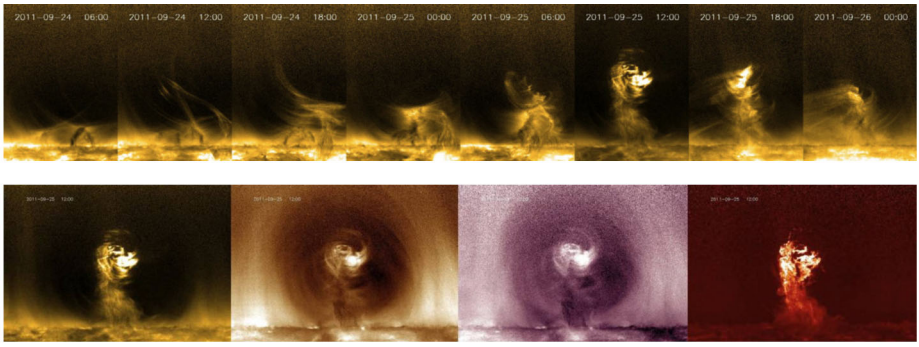

Fig. 3 Top row: evolution of a tornado prominence observed by SDO/AIA between 24 and 26 September 2011. Bottom row: the same tornado prominence in different AIA wavelength channels (171, 193, 211, and 304 Å). Adapted from Li et al. (2012)

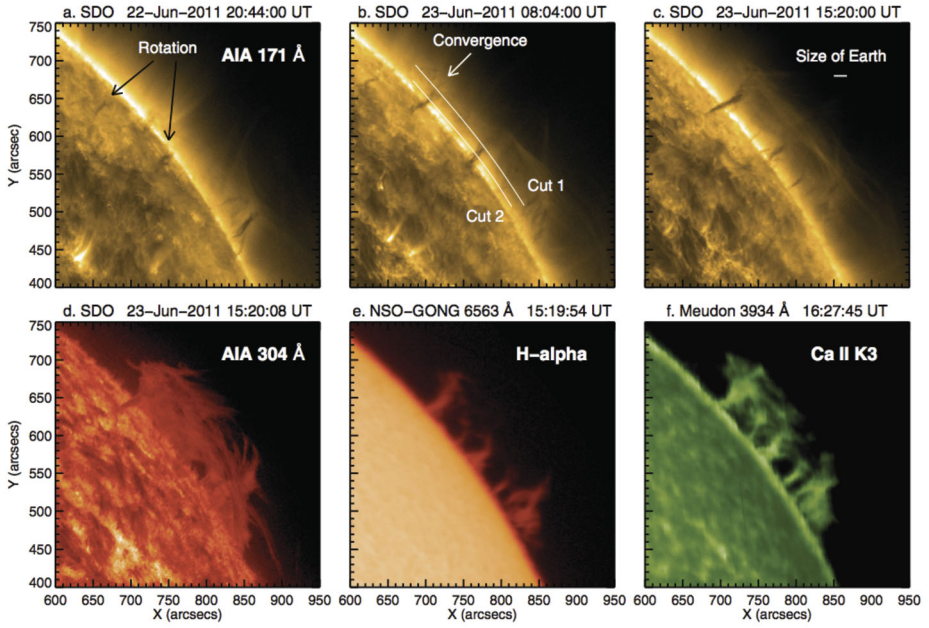

Fig. 4 A multi-wavelength view of a group of solar prominences, reproduced from Fig. 1 of Su et al. (2012). Panels (a), (b), and (c) show SDO/AIA 171 Å images at three times as the tornadoes crossed the limb. Panels (d), (e), and (f) show the corresponding images in He II 304 Å (AIA), Hα (NSO), and Ca II K (Meudon) respectively

M. Druckmüller[3] that shows a composite AIA observations of the prominence analysed by Li et al. (2012). Interestingly, this movie also shows rather stable pattern of vertical fine structures forming the vertical 'leg' of the observed prominence.

Su et al. (2012) presented an observation that was more similar to the Pettit classification of tornado prominences. These authors observed a number of column-like features in a quiescent prominence that appeared dark in coronal emission filters from AIA (see Appendix A for more details of the origin of dark prominence structures in AIA coronal filters) and found that they could be directly related to bright emission seen in Hα and Ca II (see Fig. 4). These prominence features appeared as funnels, or columns of absorbing material which were wider at their tops than at their bases. Su et al. (2012) found a clear correspondence between the dark columns of prominences that the authors named tornadoes and the barbs of filaments observed on the solar disk. This suggests that filament barbs may, at certain wavelengths and at certain projection angles, appear as isolated funnel-like structures. In this case they were visible both in emission in Hα or Ca II, and in absorption in coronal wavebands of AIA, such as 171 Å but cannot be identified in 304 Å channel (see Fig. 4). The solar tornadoes described by Su et al. (2012, see Fig. 2 therein) often exhibited quasiperiodic variations on the time scales between 10 minutes and one hour. The authors also studied the photospheric flux distributions at the feet of the filament barbs observed on the solar disk in the AIA 171 Å waveband. Using the SDO/HMI (Helioseismic and Magnetic Imager; Scherrer et al. 2012) magnetograms, Su et al. (2012) identified swirling features in the photosphere similar to those reported by Wedemeyer-Böhm et al. (2012) – see Sect. 2

[3] http://www.zam.fme.vutbr.cz/~druck/Sdo/Pm-nafe/2011_09_25/0-info.htm

or review by Tziotziou et al. (2023) for more details. Based on the presence of these photospheric swirling features, Su et al. (2012) suggested that the magnetic field might be in a twisted (or twisting) helical configuration, where plasma flowed along the field lines, giving the appearance of rotation.

Similar features and analyses have been reported by a number of authors since then. Wedemeyer et al. (2013a), for example, analysed over two hundred funnel-like absorption features visible in the 171 Å waveband of AIA. The authors call these features 'giant tornadoes' and conclude that they form "the legs of prominences". Several of the prominences studied by Wedemeyer et al. (2013a) erupted, in which case they showed signatures of helical structures and rotational motions around the axis parallel to the solar surface, similar to the event studied by Li et al. (2012). Wedemeyer et al. (2013a) also analysed the Swedish Solar Telescope (SST; Scharmer et al. 2003) observations of a prominence visible in the Hα line on June 8, 2012. The Dopplergram of this prominence (see Fig. 4 of Wedemeyer et al. 2013a) shows a pattern of line-of-sight (LOS) velocities ranging from -20 to $+30$ km s^{-1} that might be indicative of a rotation of the entire prominence leg around the vertical axis. Such a pattern of redshifts down one side of the prominence leg and blueshifts down the other was found also by Pettit (1946), albeit with much smaller LOS velocities. Unfortunately, due to unstable seeing conditions, the pattern derived by Wedemeyer et al. (2013a) is based only on the best scans making it unclear whether it was sustained for a longer time.

Such a split pattern of red and blue Doppler shifts indicative of rotational motions in prominence legs was also reported by Orozco Suárez et al. (2012). These authors analysed observations in the near-infrared He I 10830 Å line obtained by the German Vacuum Tower Telescope (VTT) and in the SDO/AIA 171 Å channel. The He I 10830 Å line dataset contains 66 minutes long time-series of single slit sit-and-stare observations with the slit that is parallel to the solar limb and crosses two legs of a hedgerow prominences (see Fig. 1 of Orozco Suárez et al. 2012). Figure 5 therein shows a sustained Doppler-velocity pattern of red-shifts on one side of the cut across one of the observed prominence leg and blue-shifts on the other side. This pattern was present for about 30 minutes, then seemed to subside or reverse for a few minutes (around minute 30) and continue for another half an hour. The typical detected LOS velocities are around ± 3 km s^{-1}, significantly lower than those found by Wedemeyer et al. (2013a) and in line with Pettit (1946). Orozco Suárez et al. (2012) did not use the term 'tornado' but concluded that the rotational velocities in the observed 'prominence feet' are similar to those inferred by Li et al. (2012) or Su et al. (2012).

While the previously described studies identified indications of rotational motions in the cool plasma of prominences, systematic Doppler velocities consistent with a rotation around the vertical axis have also been reported by Su et al. (2014) and Levens et al. (2015) in the hot plasma forming the PCTR that surrounds prominences. Both Su et al. (2014) and Levens et al. (2015) analysed the same 'prominence tornado' observed using the Extreme-ultraviolet Imaging Spectrometer (EIS; Culhane et al. 2007) onboard the Hinode satellite (Kosugi et al. 2007). Hinode/EIS provided raster scans covering the prominence in wavelength ranges of 170–211 Å and 246–292 Å that contain spectral lines formed at temperatures reaching coronal values. In both cases, the analysis of the derived Doppler-shift velocities showed a clear pattern of blueshifts on one side of the vertical prominence leg and redshifts on the other side. This split pattern was sustained for the full three hours of the available data set in the lines formed at temperatures of 1.5–2.0 MK (see Fig. 2 of Su et al. 2014) and extended down to 1.0 MK values (see Fig. 7 of Levens et al. 2015). Such a stable pattern is striking because the previous observations of similar rotational signatures in the cool prominence material are only intermittent. However, as we demonstrate in Sect. 5.1.1, it is likely that these results are due to the EIS instrument having a tipped, elliptical point spread function (PSF).

Martínez González et al. (2015) published spectro-polarimetric observations of the He I 10830 Å line in the feet of a prominence where the inversion of the polarisation data provided two solutions: one nearly vertical with the field inclination of 30 or 150 degrees with respect to the vertical, and one horizontal with the inclination of about 90 degrees. This double solution reflects one of the difficulties of using polarimetry to infer magnetic fields: several magnetic configurations may result in rigorously identical polarization profiles in a given line. The 180-degrees ambiguity is quite well-known from measurements in the photosphere with the Zeeman effect. The Hanle effect adds a 90-degrees ambiguity which is the one responsible for the two solutions in Martínez González et al. (2015). As Casini et al. (2009) demonstrated, the He line at 10830 Å is particularly sensitive to this ambiguity. In the absence of additional observations that would allow to resolve this ambiguity (see Sect. 5.3 for more details), Martínez González et al. (2015) relied on an assumption that in the magnetic field configuration of the observed prominence "there are no tangential discontinuities or shocks" and thus the magnetic field lines "draw continuous lines". This means that the magnetic field lines should be continuous within the visible (projected) volume of the prominence feet. With this assumption in place, Martínez González et al. (2015) applied the Kruskal-Shafranov stability criteria which led to the preference of the solution of the helical magnetic field with a nearly vertical orientation. However, it can be argued that the assumption of continuous field lines within a prominence volume visible in the He 10830 Å line is too strong. Firstly, the volume of the cool prominence material visible in the He 10830 Å line does not correspond to the definite extent of the observed prominence. Even in Fig. 2 of Martínez González et al. (2015) we can clearly see that the volume of this prominence visible in the Hα line is more extended than that in the He 10830 Å line. Moreover, if the authors would consider optically thick lines, such as He II 304 observed by SDO/AIA, the prominence volume in which to apply the chosen stability criteria would be far larger. That might have easily led to a preference of a horizontal solution over the helical (vertical) one. Secondly, and more importantly, 3D models of prominences, such as those of Gunár and Mackay (2015a,b), Gunár et al. (2018) or Jenkins and Keppens (2022) clearly show that prominence plasma observable in lines such as Hα occupies only a small portion of the entire volume of prominence magnetic field configurations. This is because the dense plasma of prominences is located in the dipped parts of the predominantly horizontal field while the field lines supporting this plasma extend much further and eventually connect to the photosphere. In this generally accepted scenario there is no need for the magnetic field lines to be present only within the volume of the cool prominence plasma.

A clear signature of sustained split red and blue Doppler-shift pattern indicating rotation was detected also by Yang et al. (2018) using the Interface Region Imaging Spectrograph (IRIS; De Pontieu et al. 2014) Mg II k and Si IV spectra of two 'prominence tornadoes'. In the first case, see Fig. 1 of Yang et al. (2018), the authors analysed single-slit sit-and-stare observations lasting 2.5 hours. The slit was parallel to the limb and crossed a vertical leg of an arch-like quiescent prominence. The time-distance diagrams of the LOS velocities derived from both the Mg II and Si IV spectra (see Fig. 2 of Yang et al. 2018) show a coherent pattern of blue Doppler shifts along one (outer) side of the prominence leg and mostly red Doppler shift along the inner side. Convincingly, both analysed lines provide similar values of LOS velocities which range from -12 to 12 km s^{-1}. The outer blue Doppler-shifted region seems to overlap with lower intensity profiles, which, in the case of Mg II, are also narrow and less complex. The rotational axis would be oriented almost vertically and would correspond with the vertical axis of the observed prominence leg. In the second case, Yang et al. 2018 analysed six slit positions with an inclination of about 30 degrees from being parallel to the solar limb (see Fig. 7 of Yang et al. 2018). The derived Doppler

shifts are again quite consistent between the Mg II and Si IV spectra and keep a rather stable pattern of red-shifts in the outer part of the time-distance diagram and blue-shifts in the inner part (see Fig. 8 of Yang et al. 2018) for almost 3.5 hours. Only in the inner part of the analysed diagrams, we can see fluctuations of red and blue Doppler shift patterns when we compare individual slits. Also, in this case, Yang et al. (2018) concluded that the derived LOS velocities are indicative of a rotation. The rotational axis would then have an apparent inclination of 60 degrees from being vertical, but due to projection effects it is difficult to estimate its true orientation. An alternative interpretation might be that the observed signatures correspond to helical plasma flows (perhaps siphon flows) along a more or less static helical magnetic structure around a central core, perhaps similar to the model of Luna et al. (2015) – see Sect. 6.1 for more details. However, the possibility of oppositely directed flows, with components both in and out of the plane of the sky, is not ruled out by the data. The complex Mg II h&k profiles may need deeper analysis, as done by, e.g., Schmieder et al. (2014b), where multi-component fits of Mg II h&k lines revealed interesting large-scale Doppler-shift patterns not apparent in a single-Gaussian fitting.

Naturally, this series of works raised questions about the nature of the magnetic field in these prominence tornadoes, and how the plasma could be supported against gravity. It also heightened the interest in the study of prominences and the connection between their dynamics and magnetic field configurations. This interest resulted in several observational and theoretical papers that put forward different explanations for the observed signatures similar to those described above. We review these papers and summarise their findings in Sects. 5 and 6.

However, before we review these papers, we need to mention the other rotational (or swirling) structures observed in the solar atmosphere that are not directly connected to the type of prominences studied here but are also named ‘tornadoes’. One type of tornado-like structure identified in the lower solar atmosphere – the photospheric and chromospheric swirls – we described in Sect. 2. Another example of the use of the term ‘solar tornadoes’ can be found in the works by Chen et al. (2017, 2020) and Wang et al. (2017), where the authors use it to describe helical features of eruptive prominences.

5 Different Explanations for so-Called Prominence Tornadoes: Observational Evidence

In this section, we review recent papers that explore the possibilities that the observed characteristics of so-called prominence tornadoes can be associated with other observed prominence features or dynamics, providing alternative, non-tornado-like explanations. First, we address the signatures of rotation arising from Doppler-shift analysis of LOS velocities in Sect. 5.1. Second, we investigate the apparent helical motions of prominence fine structures in the context of their true motions in the 3D space (Sect. 5.2). Third, we compare the properties of the prominence magnetic field inferred from the spectro-polarimetric observations with the notion of sustained rotation of prominence material (Sect. 5.3).

Many of the addressed counter-points to the reported observations of prominence tornadoes (Li et al. 2012; Su et al. 2012; Orozco Suárez et al. 2012) were raised already by Panasenco et al. (2014). These authors argued against the rotational tornado model and instead proposed that the observed motions can be accounted for by oscillations and counter-flows in the more traditional horizontal, dipped magnetic field. Firstly, and correctly, Panasenco et al. (2014) made a distinction between the tornadoes of Li et al. (2012) and Su et al. (2012) – morphologically they are different and the reported rotation is in a different

plane. Panasenco et al. (2014) then showed an observation from TRACE (Transition Region and Coronal Explorer; Handy et al. 1999) that indicates that vertical tornado-like features of prominences (of the Su et al. variety) correspond directly to filament barbs when viewed on disc. Further analysis of a tornado from SDO/AIA showed that the sinusoidal motion found in the time-distance diagrams can be easily explained by oscillation and counter-streaming of prominence plasma in a horizontal magnetic field. Panasenco et al. (2014) stated that the observed 'rotation' is simply an optical illusion created by the projection of these oscillations onto the plane of the sky and that the Doppler pattern reported by Orozco Suárez et al. (2012) was a misinterpretation of counter-streaming flows. The tornado of Li et al. (2012) was explained by Panasenco et al. (2014) as the motion of plasma along a writhed magnetic field, viewed in projection.

5.1 Doppler-Shift Signatures: Oscillations, Waves, and Flows

It is a well-known fact that the fine structures of even the most stable quiescent prominences exhibit continuous dynamical changes with velocities of the order of 10 km s^{-1}. Such dynamical behaviour is further enhanced in the active or eruptive prominences. The sources of the prominence dynamics range from plasma flows along the field lines that often show an opposite direction in nearby regions (so-called counter-streaming flows, see, e.g., Schmieder et al. 1991; Zirker et al. 1998; Lin et al. 2003, 2005; Chae et al. 2005), oscillations of the prominence fine structures due to external triggers (Okamoto et al. 2007, 2015; Schmieder et al. 2013, 2014; Zapiór et al. 2015; Luna et al. 2018; Arregui et al. 2018), displacements of the prominence plasma (or magnetic field hosting the plasma) due to instabilities (Berger et al. 2008; Jenkins and Keppens 2022), reconnection (Okamoto et al. 2016) or passing waves (Antolin et al. 2015; Ofman et al. 2015). All of these motions, often visible in plane-of-the-sky movies, naturally have also a line-of-sight component that is routinely detected as Doppler shifts in the spectral observations. Because the observed motions of prominence fine structures are often incoherent, it is also natural to obtain various (and varying) patterns of Doppler shifts in prominences. As we demonstrate in this section, to reliably interpret a Doppler-shift pattern as an undisputable sign of a rotational movement, we need long-duration spectroscopic observations in more than just a single slit position. Even then, we also need to detect relatively large sustained rotational speeds to overcome the uncertainties inherent in the Doppler-shift measurement method – see Sects. 5.1.2 and 5.1.3 and Appendix B.

Observable signatures of all these forms of prominence dynamics may be very similar to the signatures of rotation, especially when we rely on the Doppler-shift analyses. This fact causes significant ambiguities when interpreting the observations of seemingly rotating prominences, opening doors to other, non-rotating, explanations. For example, Mghebrishvili et al. (2015) studied a slowly rising prominence showing a typical arch-like structure with underlying vertical prominence barbs – column-like structures visible in absorption in coronal AIA 171 Å channel (see Appendix A for more details of the origin of dark prominence structures in AIA coronal filters). These authors analysed detailed dynamics in one of the prominence legs and reported a pattern of "quasi periodic transverse displacements" which, they hypothesized, could be attributed to either MHD kink waves or to two individual strands of cool prominence material twisting around a common vertical axis. Later, Mghebrishvili et al. (2018) published an interesting statistical analysis of the connection between the onset of Coronal Mass Ejections (CMEs) and the occurrence of column-like vertical features ('tornadoes' of Su et al. variety) in prominences visible in absorption in the AIA 171 channel. These authors visually identified all "prominence tornadoes" observed

by SDO/AIA over the year 2011 and analysed their life-times. Although there is no observational evidence of rotational motions in the studied tornado-like structures, the authors presented strong indications that the presence of these structures in the AIA 171 observations is connected with prominence eruptions and subsequent CMEs. While this connection does not confirm a causality between the existence of 'prominence tornadoes' and the loss of prominence stability, it points towards an interesting possible precursor to CMEs.

The ambiguity in the interpretation of the LOS velocity patterns arises also in the work of Martínez González et al. (2016). These authors used spectro-polarimetric observations of a quiescent prominence in the He I 10830 Å line obtained by VTT. The observed data set contains four scans, each taking around 30 minutes. As is clear from Fig. 5 of Martínez González et al. (2016), a large-scale, vertically split red and blue pattern of Doppler-shift velocities is present only in the second and the third scan, and even then the pattern is reversed in the third scan compared to the second. Martínez González et al. (2016) thus conclude that "if rotation exists, it is intermittent, lasting no more than one hour" but "the observed velocity pattern is also consistent with an oscillatory velocity pattern".

The incoherence that Martínez González et al. (2016) found in the Doppler-shift patterns is likely a typical feature of prominences. This is clear, for example, from the work of Schmieder et al. (2017a), who analysed observations of a quiescent prominence obtained in Hα by the Multi-channel Subtractive Double Pass (MSDP) spectrograph at the Meudon Solar Tower (Mein 1991). MSDP provided Dopplergrams with a cadence of 30 seconds over a two hour period. In Fig. 5 we show two typical LOS velocity maps with the range of velocities between -3 and 3 km s^{-1}. Large cells of blue-shifts and red-shifts with sizes of about 5-10″are changing over time and reversing the LOS velocity signs (from blue to red-shift and vice versa) with a quasi-periodicity of about 40 to 60 minutes (Schmieder et al. 2017a). When cuts parallel to the limb are taken at various heights and the time-distance diagrams of Doppler shifts are plotted (see the bottom panels of Fig. 5), we can see very different

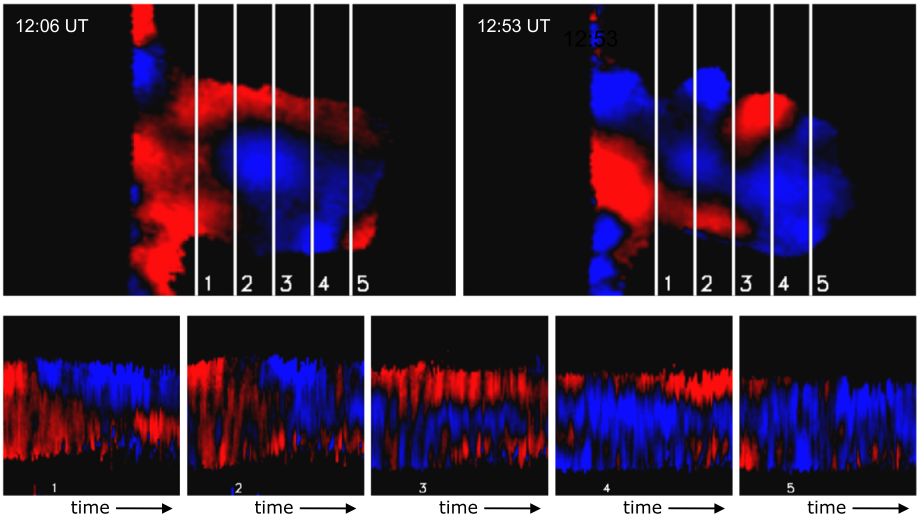

Fig. 5 Evolution of the Doppler-shift pattern in a quiescent prominence observed in Hα with the MSDP spectrograph operating at the Meudon solar tower. The top panels present two LOS velocity maps with the solar limb oriented vertically. The numbered lines are the slits along which the time-distance diagrams displayed in the bottom panels have been computed. Adapted from Schmieder et al. (2017a)

'evolutions' of the Doppler shifts created simply by chance. Some of these time-distance diagrams may show the split red and blue Doppler-shift patterns sustained for about an hour. However, these arise purely by coincidence and do not exist in parallel co-temporal cuts just a few thousand km above or below. These coincidental and localised signatures cannot be taken as an unequivocal sign of a sustained rotation of entire structures. Schmieder et al. (2017a) explained the quasi-periodicity in the Doppler shift maps as being oscillations of the dipped magnetic structure sustaining the prominence plasma. Split Doppler shifts were also detected in (mostly active) prominences by Kupryakov et al. (2019).

No evidence of rotational movement was found by Kucera et al. (2018) who performed a detailed study of motions in a barb of a quiescent prominence. The authors analysed almost 4 hours of coordinated IRIS Mg II h&k and Hinode/SOT (Solar Optical Telescope; Tsuneta et al. 2008; Suematsu et al. 2008) Ca II and Hα observations. Although the derived Doppler shifts revealed line-of-sight motions in the cool prominence material forming the barb, these were transitory and localised. They thus could be taken neither as a clear signature of rotation nor as a "sign of persistent large-scale flows". Instead, Kucera et al. (2018) concluded that the observations suggest "a complex environment in which large-scale motions are more consistent with either motion of discrete structures making up the barb or oscillations of some sort". Kucera et al. (2018) show that the Doppler images derived from the Mg II spectral rasters were complex because of multiple features along the line of sight, but again no systematic rotation was revealed by either fits to Mg II h&k lines with a single or double Gaussians.

Levens et al. (2016a, 2017) investigated multi-instrument coordinated observations of a quiescent prominence showing two dark pillar-like structures in SDO/AIA coronal channels. In the AIA 171 Å channel, the authors detected quasi-periodic oscillations similar to those observed by Schmieder et al. (2017a) in AIA 193 Å channel. These oscillatory movements may be caused by passing waves or, on their own, might be taken as a sign of rotation. Analysis of Doppler shifts from IRIS Mg II k spectra, however, does not show any persistent pattern consistent with rotation (in contrast to Yang et al. 2018). Moreover, THEMIS spectro-polarimetric observations (see Sect. 5.3 for more details) show that the magnetic field in both prominence legs is predominantly horizontal (Fig. 6 of Levens et al. 2016a), which is also inconsistent with a persistent rotation of prominence material around a vertical axis.

The signatures of LOS velocities and rotational motions in a quiescent prominence were analysed also by Barczynski et al. (2021) using Hα and Mg II h&k observations. These authors concluded that the observed Doppler-shift patterns, together with the analysed fine-structure movements at the active top of the prominence (referred to as 'tornado') are indicative of counter-streaming flows rather than a sustained rotation.

5.1.1 Observations by Hinode/EIS: The Role of a Chromatic PSF

In Sect. 4, we describe the striking observations of a long-duration stable pattern of split red and blue Doppler shifts in the hot PCTR plasma reported by Su et al. (2014) and Levens et al. (2015). However, as we demonstrate here, it is likely that this Doppler-shift pattern is a result of the instrumental effects caused by the chromatic PSF of Hinode/EIS. This has been discussed in the context of other coronal observations by the EIS instrument team (Young et al. 2012; Warren et al. 2018). For data from a spectrometer with such a PSF, a sharp intensity gradient produces an apparent Doppler shift. A thin, elongated dark feature against a bright background aligned across the slit direction would show a Doppler shift in one direction on one side and the opposite direction on the other. In Fig. 6 we show the results

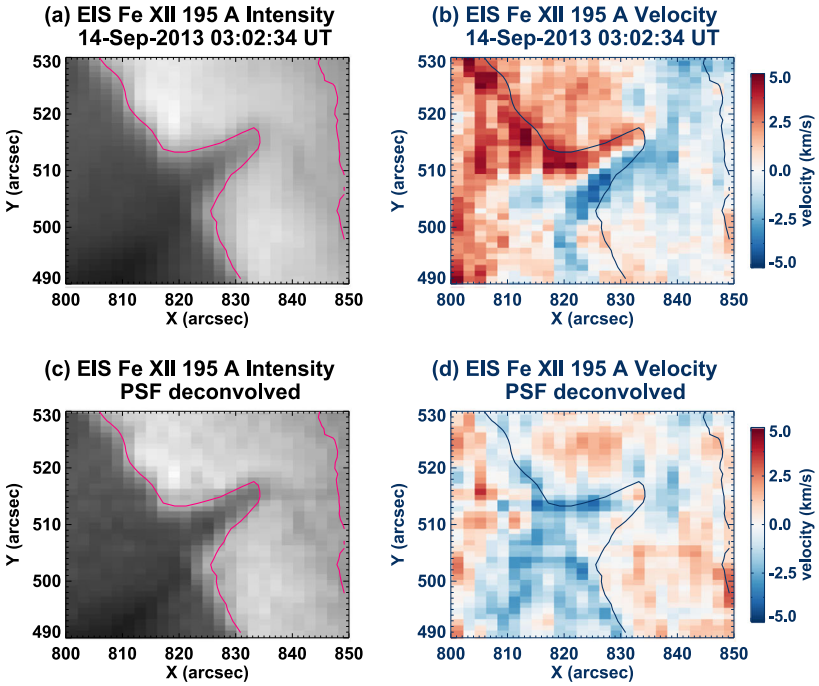

Fig. 6 Line intensity and Doppler velocity calculated using a one-Gaussian fit to the Fe XII line at 195.12 Å (a–b) using the standard data pipeline, (c–d) after deconvolving the data with the EIS PSF function used in Warren et al. (2018). The contours are from the intensity map in panel (a). The PSF deconvolution completely removes the apparent rotation signature seen without the deconvolution

of a one-Gaussian fit to the Fe XII line at 195 Å. The top row shows intensity and Doppler velocity derived from the original data. The bottom row shows the same quantities measured after the PSF used in Warren et al. (2018) has been deconvolved from the data. After the PSF is deconvolved the 'tornado' effect completely disappears. Fitting the deconvolved data with two Gaussians (for the blended Fe XII lines at 195.119 and 195.179 Å) gives essentially the same result. As discussed in Warren et al. (2018), the exact form of the PSF is still uncertain. However, this demonstrates that the shifts shown in the 2013 September 14 prominence observations are not reliable and are consistent with this instrumental effect.

5.1.2 Relationship Between LOS Velocities Derived from Doppler Shifts and the True LOS Velocities

It is important to remember that velocities derived from Doppler shifts do not always provide true information about the LOS component of the velocity of the observed plasma structures. This is caused by several factors, among which the most important is the optical thickness of the observed plasma in the used spectral line.

In the optically very thick case, the observed spectral line is produced in a narrow region closest to the observer. This means that the Doppler shift of such a spectral line provides information about the true LOS velocity of that particular region. However, we do not gain any insight into the movement of the plasma beyond this region unless the spectral line in question is narrow and thus very sensitive to the velocity. Then we can obtain complex

profiles with a contribution from deeper regions due to mechanisms described in detail in Appendix B. Such complex, often strongly asymmetric, reversed or even multi-peaked profiles (see, e.g., Ruan et al. 2018; Tei et al. 2020) pose another problem for the determination of the true LOS velocities. This is because the Doppler shifts of complex line profiles do not convey information about the absolute LOS velocity of the foremost, or any other individual plasma structure, but of a superposition of all of them. Therefore, if such an asymmetric profile is analysed in the context of a single moving plasma structure, the obtained Doppler-shift velocity does not provide a truly correct measurement. The difference between the true LOS velocities of individual plasma structures and the apparent Doppler-shift velocity derived from their superposition may be significant. Moreover, in typical prominences we can see a mix of simple and complex profiles (see, e.g. Ruan et al. 2018; Yang et al. 2018) which likely arise from a complex situation where we either see single structures or multiple moving structures in different pixels. That may easily lead to scenarios where the simple profiles provide information about the true LOS velocity of individual, randomly moving fine structures while the Doppler shifts of the complex profiles exhibit fluctuating apparent LOS velocities that may not be at all representative of any true LOS velocities of the multiple moving fine structures present along the given line of sight. As is clear from such a scenario (see Sect. 6.2 for more details), the simple profiles arising from single moving fine structures are likely to be present preferentially at the boundaries of the observed prominences while the complex profiles probably come from the central parts. Such a scenario might provide an alternative explanation to the Doppler-shift patterns observed by Yang et al. (2018).

In the optically thin case, the information about the LOS movement of all plasma structures propagates through the entire observed medium and is integrated into the final spectral line profile. This means that the resulting profile either provides information about the true LOS velocity of a homogeneous medium or contains a superposition of Doppler shifts from all individual plasma structures moving with different LOS velocities. If these structures move with sufficiently different LOS velocities (producing Doppler shifts comparable to or larger than the full width at half-maximum of a single structure) we will observe clearly separated individual spectral line components. We are then able to derive the true LOS velocities of individual plasma structures. However, if these structures move with LOS velocities which do not cause sufficiently large Doppler shifts, the resulting profile will be broadened and generally asymmetric. In such a case, we can imagine a simple scenario in which two identical plasma structures move with equal but opposite LOS velocities. The resulting spectral profile would be symmetric and centred at the rest wavelength, which would lead us to assume that we observe a single, stationary plasma structure while we are observing two structures with potentially significant opposite LOS velocities. Such a scenario was discussed by Gunár et al. (2012). Of course, due to a large number of dynamic fine structures forming prominences, the real situation is even more complex than this simple example.

As we briefly demonstrate in this section, it is important to understand that the information about the LOS velocities derived from Doppler shifts is not always robust. This is true regardless whether we use optically thick or thin spectral lines.

5.1.3 Determination of the True Rest Velocity

A special caution should also be paid to the question of determination of the true zero (rest) wavelength of a spectral line. This is often not straightforward because it depends on instrumental factors and thus it may carry sizeable errors. While errors of a few km s^{-1} may be negligible when we observe motions with LOS velocities of the order of few tens of km s^{-1}, if we interpret measurements of LOS velocities of a few km s^{-1}, the errors in the rest velocity determination may clearly have a profound impact. That is especially true when we

analyse signatures of rotation. For example, in the case of Doppler shifts on the order of ± 3 km s^{-1}, such as those of Orozco Suárez et al. (2012) or Schmieder et al. (2017a). In such a case, the uncertainty of a few km s^{-1} in the rest velocity may change a measurement showing rotation with -3 km s^{-1} on one side, 0 km s^{-1} in the middle (axis) of the observed structure and 3 km s^{-1} on the other side into a signature of a movement of -6 km s^{-1} on one side and 0 km s^{-1} on the other side. While this difference may seem small, the interpretation of such observations could differ between clear sign of a rotation and a non-uniform translation, expansion, or contraction.

5.2 Prominence Fine Structure Motions in 3D Space

As we already discussed, prominence fine structures exhibit a broad range of movements which are clearly visible in high-resolution movies. However, the plane-of-the-sky movements, such as down-flows, up-flows or movement along seemingly circular or helical trajectories, do not paint the whole picture. This is because the plane-of-the-sky components of the velocity vector, which our brains intuitively recognize in the movies, are not the only components of the full velocity vector of the observed fine structures. Indeed, these perceived movements are often subordinate to the movements happening along the line of sight which are hidden in the movies. Thus the seemingly rotational movements, which we instinctively see in high-resolution movies such as those from SDO/AIA, have alternative, more likely explanations. Therefore, unequivocal confirmation of tornado-like dynamics (coherent and sustained rotation around a vertical axis) of large-scale prominence structures needs to be supported by careful analysis of all possible explanations.

One of the examples of this general characteristic of prominence fine-structure dynamics is shown in the work of Schmieder et al. (2010). These authors analysed coordinated observations of a quiescent prominence obtained by Hinode/SOT and the MSDP spectrograph at the Meudon Solar Tower. Employing the time-slice technique for the Hinode/SOT movies and the Doppler-velocity determination for the 2D MSDP spectra, Schmieder et al. (2010) demonstrated that in most places in the observed prominence, the perceived plane-of-the-sky velocities typically have a LOS component with a similar amplitude.

Even the downward motions of prominence fine structure, which are often seen in high-resolution movies, do not need to contradict the existence of the predominantly horizontal magnetic field in prominences. This was indicated, for example, by Chae (2010), who analysed a quiescent hedgerow prominence observed by Hinode/SOT. Chae (2010) showed that the falling prominence fine structures, even those with apparent downward velocities of up to 30 km s^{-1}, typically undergo negligible vertical acceleration. This indicates that even during the descending phase, prominence fine structures are being supported against gravity by the horizontal magnetic field. The complex variations of their descending speeds could then be attributed to small imbalances between gravity and the force of magnetic tension and to the local reconnection events.

The investigation of the true velocity vectors in the 3D space was further extended by Schmieder et al. (2017b), who reconstructed 3D trajectories of individual fine structures of a quiescent prominence observed by IRIS and Hinode/SOT during a coordinated observing campaign. In the plane-of-the-sky projection the prominence exhibited an apparent helical structure (around a horizontal axis) with individual knots of prominence plasma moving along seemingly elliptical trajectories – see Fig. 7. However, Schmieder et al. (2017b) also derived the full velocity vectors for several dynamic knots following their evolution. To do so, the authors used a method for reconstruction of velocity vectors in 3D (Zapiór and Rudawy 2012; Zapiór and Martínez-Gómez 2016) which combines measurements of the

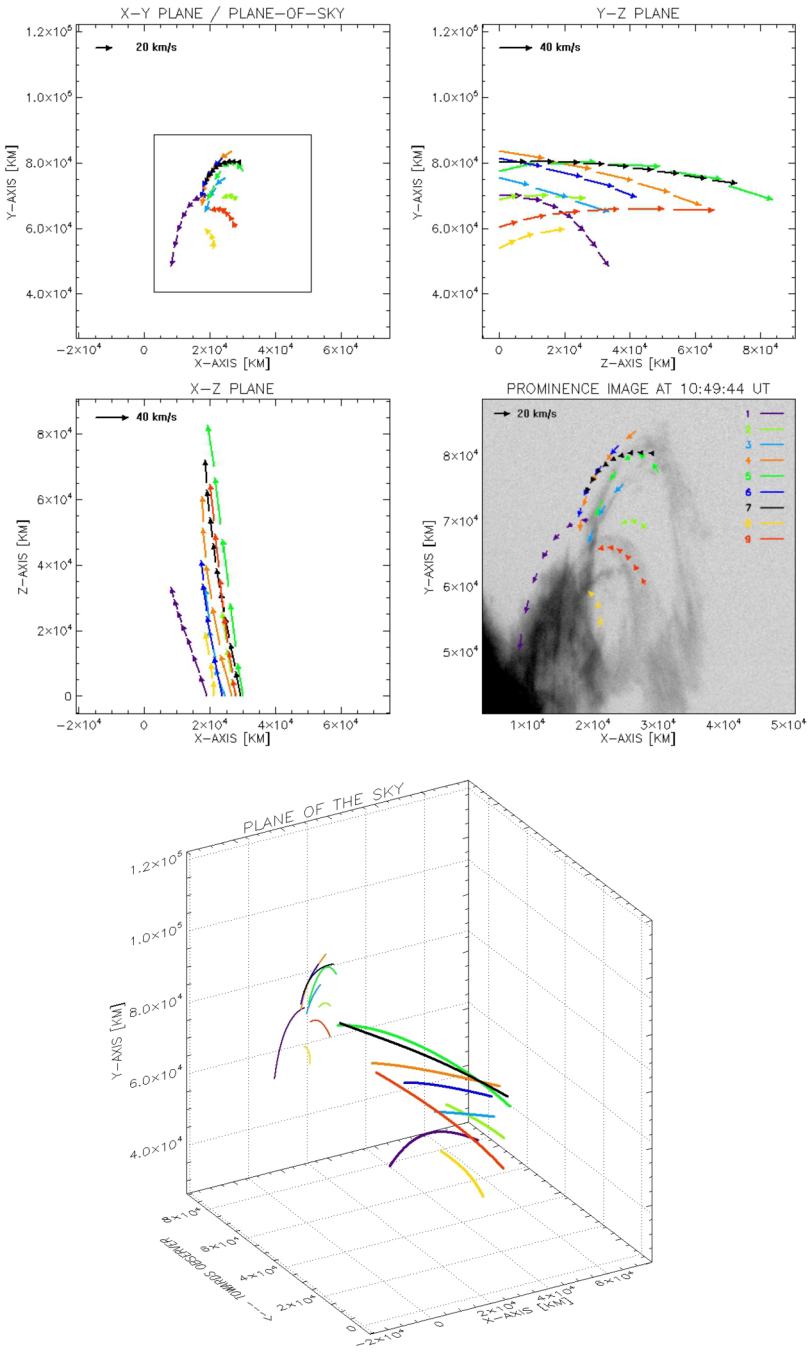

Fig. 7 3D reconstruction of cool knots trajectories along an helicoidal prominence observed with IRIS projected on three planes x-y, x-z, y-z. Adapted from Schmieder et al. (2017b)

plane-of-the-sky positions and the line-of-sight Doppler velocities of individual prominence fine structures. For a given time interval, a shift of the position of the centroid (centre of gravity) of individual knots was derived from IRIS slit-jaw images and combined with the shift along the LOS calculated from the Doppler velocities. Since the starting positions of the knots along the LOS are not known, the derived 3D trajectories may be shifted by any arbitrary value along the LOS, but their true 3D shape is conserved. In Fig. 7, we show the restored 3D trajectories which do not exhibit any helical structure. They are elongated in the direction of the LOS and nearly parallel to the solar surface. Note that the shapes of all restored trajectories are similar, which indicates the robustness of the used reconstruction method. It is only the projection effect which gives an impression of a helical structure in the plane of the sky.

The understanding of the true movement of prominence plasma in 3D space therefore has a strong impact on the interpretation of helical or cyclonic dynamics in prominence observations such as those of Li et al. (2012). This is because in cases when we are seeing prominence structures along the axis of the flux ropes we are likely subjected to very strong projection effects. These make the natural movement of prominence plasma along predominantly horizontal magnetic field lines appear as a cyclonic movement of prominence fine structures. This discrepancy in the perceived and true dynamics of observed prominence plasma can be better understood when we look at the 3D configuration of the prominence magnetic field and its significantly varying projections into different observing planes – for more details see the model of Gunár et al. (2018) discussed in Sect. 6.4.

5.3 Magnetic Fields Inferred from Prominence Dynamics and Spectropolarimetry

In principle, the dynamics of prominence fine structures observed in high-resolution movies can be used to infer the topology of prominence magnetic fields. This is justified by the low β value of plasma in prominences. The ionised plasma can thus be safely considered as attached to the field lines, which means that its movement along the field is easy while the movement across the field is difficult or impossible. This statement has to be qualified because it is known that prominences are only partially ionised, being composed of a combination of neutral atoms and ions. In general, neutral atoms such as He I or H I are not tied to the magnetic field. They are assumed, however, to be temporary states of their ionised counterparts either due to the high temperatures outside the prominence or due to photoionization. Even then, some diffusion is to be expected, but the estimated and observed velocities of such diffusion of the neutrals with respect to the magnetic field (see, e.g., Gilbert et al. 2002, 2007) are too low to explain the observed prominence dynamics. Nevertheless, as we discussed above, the perceived movements in prominences are inevitably subjected to varying degrees of projection effects. That means that the inference of the magnetic field topology from the prominence dynamics alone may be highly unreliable without additional independent measurements.

The most obvious kind of such measurements is the spectro-polarimetric observations from which the orientation and strength of the field can be inferred. At present, the two lines of He I at 10830 Å and 5873 Å (usually referred to as D_3) are the preferred lines for prominence observations. The polarization of these lines is affected by the magnetic fields through two different phenomena: the Hanle effect (mostly modifying linear polarization) and the Zeeman effect (introducing circular polarization). Because of the relatively weak fields of prominences, it is the Hanle effect that produces the larger signals, though it has been pointed out by Casini et al. (2005) that observing circular polarization and the Zeeman effect is critical to a reliable inference of the magnetic field vector. One of the difficulties

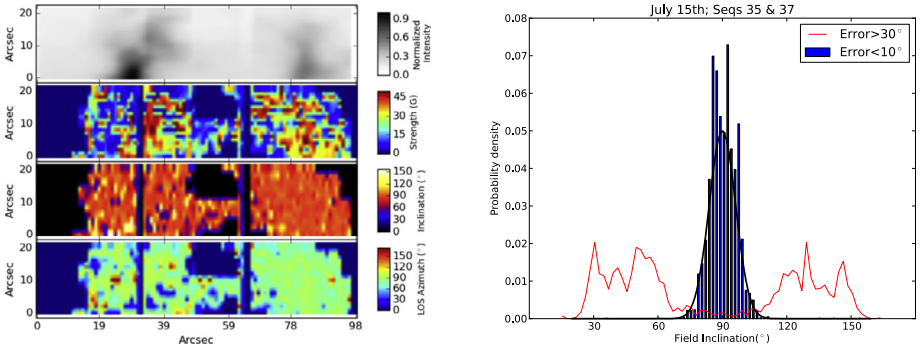

Fig. 8 Left: Magnetic field maps of a tornado observed by THEMIS on July 15th, 2014 using the He D_3 line. From top to bottom, maps of field strength, inclination respect to the local vertical and azimuth in the plane of the sky are shown. Right: Histograms of the inclination respect to the local vertical. Blue bars are pixels where the inference error is less than 10 degrees; the red line is made with pixels where the inference is larger than 30 degrees. Adapted from Levens et al. (2016a)

arising during the inference of the magnetic field vectors from polarimetric observations is the inherent ambiguities affecting the results. The 180-degree ambiguity in measurements with the Zeeman effect is well known. In the presence of the Hanle effect, a new 90-degree ambiguity is also possible between solutions symmetric with respect to the Van Vleck's angle (López Ariste and Casini 2005). As we discussed in Sect. 4, this ambiguity is responsible for the two conflicting solutions in Martínez González et al. (2015) because the He 10830 Å line is particularly sensitive to this ambiguity (see Casini et al. 2009). One way to distinguish between such ambiguous solutions is to observe using a second line whose ambiguities behave in a different manner. The He D_3 line is a particularly good candidate. However, multi-line spectropolarimetric observations in prominences are mostly unavailable at present.

From the very first use of the Hanle effect as a diagnostic of prominence magnetic fields, the existence of clearly horizontal fields supporting the plasma has been the norm (see, e.g., López Ariste et al. 2006). These measurements are in agreement with the theoretical models of magnetic topologies capable of stably supporting the prominence plasma against gravity in the solar atmosphere. While this basic paradigm has been put in doubt by the observations of vertical prominence fine structures, these were nevertheless measured to have horizontal fields. This can be explained either by the projection effects of a large 3-dimensional structure onto the plane of the sky or by pile-ups of plasma over field lines stratified in height. The same is likely true for the so-called prominence tornadoes. While the plasma in these column-like structures may appear to be aligned along helical trajectories or even moving along them, careful measurements of the magnetic fields in them show predominantly horizontal magnetic field topology. For example, measurements by Levens et al. (2016a) using the He D_3 line (which is less sensitive to the 90-degrees ambiguity) show that in those parts of the observed prominence where errors in the inclination of the field are smaller than 10 degrees, the measured field is unambiguously horizontal (see right plot of Fig. 8). While the inherent ambiguities may be part of the explanation of the large errors in other parts of this prominence, another explanation was found by Levens et al. (2016b). These authors showed that the measured vertical field inclinations with large error bars could be explained by a two-component magnetic field in the prominence: a background horizontal field on top of which a turbulent or random field was added. The resulting profiles could not

be correctly reproduced by the inversion code, which was limited to a single magnetic field vector, and the code converged towards a solution at high inclinations but with large error bars. In summary, when measurements had small error bars, the field was horizontal. Vertical fields were always associated with large error bars of more than 30 degrees, probably as the reaction of the inversion algorithm to a background horizontal field plus a turbulent or chaotic field, both contributing to the measured polarization. Levens et al. (2017) went a little further and masked off all measurements outside of the 'tornado' regions in one particular prominence simultaneously observed with IRIS and AIA. In the 'tornado' the predominance of horizontal, low-error fields over vertical large-error ones is even larger.

6 Different Explanations for so-Called Prominence Tornadoes: Theoretical Models

In this section we consider models that both support and refute the idea of rotational motions in the so-called prominence tornadoes. We also present arguments that quantify the conditions under which rotational motions in prominences may arise.

6.1 Modelling of the Twisted Magnetic Field and Rotating Plasma of Prominence Tornadoes

As we describe in Sect. 4, Su et al. (2012) suggested that 'prominence tornadoes' have a twisted magnetic structure with plasma flowing along the magnetic field lines. Based on these suggestions, Luna et al. (2015) proposed a theoretical model to explain such 'tornadoes' associated with prominence barbs. These authors argued that with the combination of vortical motions and the frozen-in condition, the magnetic field adopts a helical geometry, with almost-vertical field lines close to the rotation axis (see Fig. 9). In this configuration gravity is almost aligned with the magnetic field. The magnetic Lorentz force is always perpendicular to the field and thus almost perpendicular to gravity. In this situation the heavy prominence mass can fall down to the solar surface. The authors investigated under which conditions the prominence mass can be supported against gravity.

The model bears many similarities to astrophysical plasma jets in which the magneto-centrifugal forces collimate and accelerate the plasma. The structure of the modelled prominence is assumed stationary and axisymmetric around the vertical direction. Cylindrical

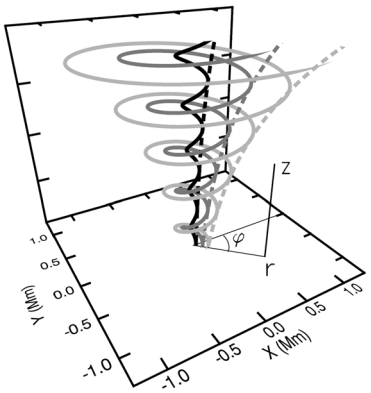

Fig. 9 Schematic picture of a tornado-like magnetic structure (see Luna et al. 2015). Solid lines are the three-dimensional representation of the magnetic field lines. Dashed lines are the poloidal field lines in the plane $\varphi =$ constant

coordinates (r, φ, z) are used, with z coinciding with the rotation axis. All the magnitudes can be decomposed in poloidal (in the rz-plane) and azimuthal (φ-direction) components. In a stationary regime there must be force balance between magnetic forces, pressure gradient, gravity and centrifugal terms. However, pressure-gradient cannot contribute to the support of the plasma against gravity. The reason is that for cool prominence plasma the pressure scale-height is too small to balance gravity in barbs as tall as those observed. In this situation the support comes exclusively from magnetic and inertial forces.

The authors computed the relevance of the centrifugal acceleration in contrast with the gravity and obtained,

$$\frac{r\,\Omega^2}{g} \approx 0.06\,, \tag{1}$$

where Ω is the angular velocity of the 'prominence tornado' at radial distance r, and g is the solar gravity. The values for r and Ω were obtained from Su et al. (2014). The ratio of Equation (1) shows that the centrifugal force cannot balance the gravity. The only way to have centrifugal support of the plasma is then for the field lines to be almost horizontal.

However, allowing for flows in the poloidal direction a new force appears along the poloidal field lines: the projection of the Lorentz force. Poloidal flows are plasma motions along the poloidal field lines. In a 'prominence tornado', the poloidal direction is almost parallel to its axis and these flows resemble the motion of the water in a fountain. This extra force depends on the poloidal velocity, v_p, the angular velocity Ω and the twist of the magnetic field structure, $B_\phi / r B_p$. Luna et al. (2015) found that it is actually possible for the magnetic force to support and accelerate the cool barb plasma against gravity along the axis of the prominence tornado under the condition

$$\frac{B_\phi}{B_p}\frac{v_\mathrm{p}}{r\,\Omega} \gg 1\,. \tag{2}$$

This relation implies that the structure of the 'prominence tornado' would need to be highly twisted and/or significant poloidal flows would have to be present. Assuming that the poloidal field lines form 60° to the horizontal and that the poloidal flux is not much larger than the rotational velocity we get that B_ϕ / B_p is larger than 4. However this ratio can be much larger depending on the mass distribution along the lines. Thus, the combined poloidal and azimuthal magnetic field would form about 14° or less with the horizontal indicating a very twisted field.

6.2 Movements of Multiple Fine Structures Creating Rotation-Like Doppler-Shift Patterns

As we describe in Sect. 5, Doppler-shift patterns resembling a rotation can be plausibly explained by motions of prominence plasma due to oscillations or counter-streaming flows. This likely explanation was presented already by Panasenco et al. (2014) and corroborated by, e.g., Martínez González et al. (2016) and Schmieder et al. (2017a) using Doppler-shift observations. Naturally, the movements of prominence fine structures caused by oscillations are not coherent for long periods and can only intermittently lead to the split red-and-blue Doppler-shift signatures of a rotation. From the results of Schmieder et al. (2017a) and the survey by Luna et al. (2018a) we can see that prominence oscillations exhibit typical quasi-periodicities of around one hour and that such oscillations are quite common. Interestingly,

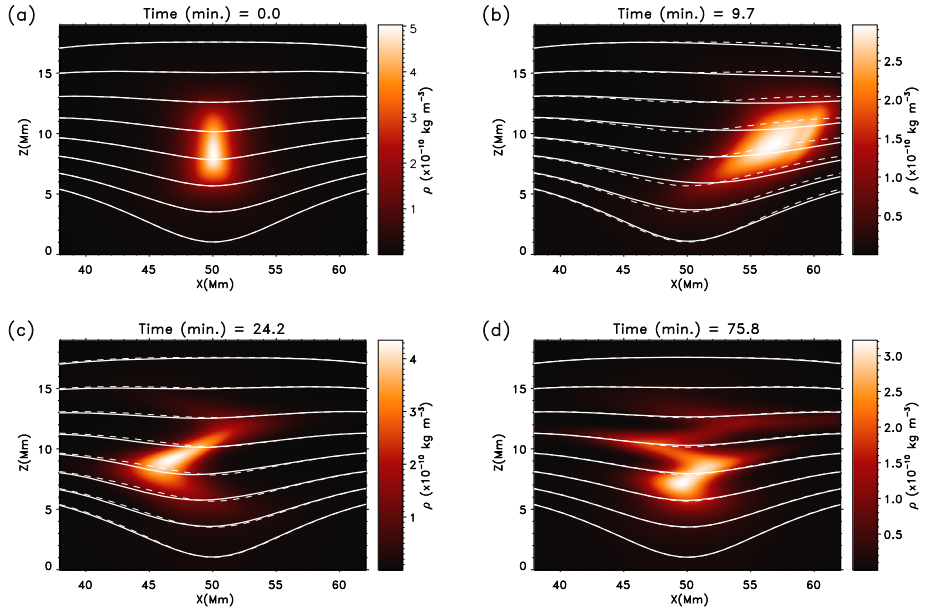

Fig. 10 From Luna et al. (2016) showing time-sequence evolution of the plasma density (colours) and the magnetic structure (white lines) at four times. Panel (a) shows the initial configuration at t = 0 when the longitudinal perturbation is applied. In (b) we see the prominence almost reaching the maximum elongation of its displacement. In (c) the phase differences between different parts of the structure is clear. In (d) a clear zig-zag motion of the prominence is shown

these periodicities are in agreement with the quasi-period variations exhibited by the 'solar tornadoes' reported by Su et al. (2012).

To understand the mechanisms of the prominence fine structure oscillations, Luna et al. (2016) constructed a gravito-acoustic oscillations model with motions of the fine-structure plasma along the dipped prominence magnetic field. These oscillations are associated with the projected gravity in the magnetic dips where the prominence resides with a small contribution of the gas-pressure gradients (Luna et al. 2012a; Luna et al. 2012b; Zhang et al. 2013). The model is also called the pendulum model because the motion of the oscillating prominence fine structures resembles a pendulum where the radius of curvature of the magnetic dip plays the role of the rod length. Luna et al. (2016), and later Liakh et al. (2020, 2021), showed that the plasma at each field line moves more or less independently and with its own period. This produces phase differences between the oscillating fine structures and a zig-zag shape of the prominence (see Fig. 10). Similar phase differences between different heights in the prominence were also found by Zhou et al. (2018) using 3D simulations of a realistic prominence configuration. This means that even when entire prominences are disturbed uniformly by external large-scale events (see, e.g., reviews by Tripathi et al. 2009 and Luna et al. 2018a) their individual fine structures, which are located in generally non-uniform magnetic dips, would naturally oscillate out of phase.

Based on these simulations, we can imagine a simple yet realistic scenario where multiple fine structures move or oscillate along magnetic field lines in the way drawn in Fig. 11. Such a scenario could easily arise in configurations with multiple fine structures where these structures do not move identically (see, e.g., Gunár et al. 2008, 2010) either due to non-coherent oscillations or counter-streaming flows. Therefore, the scenario shown in Fig. 11

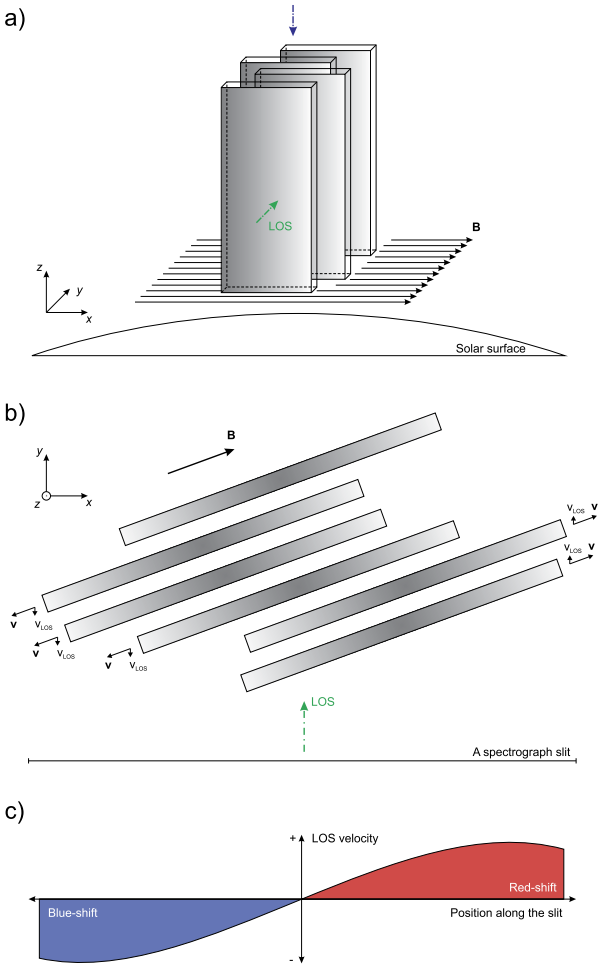

Fig. 11 Panel a) shows a sketch of a configuration of multiple 2D vertical fine structures (threads). Panel b) shows a projection of such a multi-thread configuration onto the horizontal x-y plane. The velocities of individual fine structures in the direction of the magnetic field and their projections into the LOS are denoted by arrows. Panel c) shows a sketch of the Doppler-shift signal obtained along the slit drawn in panel b)

could happen essentially randomly and relatively often. If we would observe such a configuration with a line of sight that is not perpendicular to the direction of the magnetic field (as in panel b of Fig. 11), a fraction of the velocity along the field lines would be projected into the LOS. Spectral observations of such a configuration in a line which is more-or-less optically thin (such as Hα in prominences) would yield a Doppler-shift pattern that would have dominant red-shift at one end and blue-shift at the other end (such as in the sketch in panel c of Fig. 11). In the middle of the slit where the signal from many fine structures is integrated along the LOS, the resulting Doppler shift is near zero (see Appendix B for more details).

Of course, the scenario sketched here is merely a snapshot of a configuration in which individual fine structures can, in essence, move randomly. However, with the typical oscillatory periods of around one hour, conditions leading to distinctly red-blue Doppler-shift patterns could possibly last for several tens of minutes. Observations that would steadily show the red-blue Doppler-shift patterns for such periods of time could then easily be misinterpreted as signs of a rotation. Clearly, such red-blue patterns would arise only occasionally in the non-rotating configurations. Most of the time, the obtained patterns would exhibit more

mixed Doppler-shift signals, which are, in fact, typically observed (see, e.g., Gunár et al. 2012; Zapiór et al. 2015; Schmieder et al. 2017).

We need to note here, that the split Doppler-shift patterns lasting for several tens of minutes cannot explain the stable red-and-blue patterns present in the Hinode/EIS observations reported by Su et al. (2014) and Levens et al. (2015). However, these observations are strongly affected by instrumental artefacts, as we describe in Sect. 5.1.1.

6.3 Morphological Changes Causing a Semblance of a Rotation

Changes in the prominence morphology may occasionally evoke a semblance of rotational motions projected onto the plane of the sky. This can be demonstrated by the results of Gunár and Mackay (2015b). These authors studied the evolution of both prominences and filaments using the 3D Whole-Prominence Fine Structure (WPFS) model. The 3D WPFS model, developed by Gunár and Mackay (2015a), follows the evolution of the prominence and filament fine structures caused by the changes in the underlying photospheric magnetic flux distribution. The plasma of the modelled fine structures is located in dips of the magnetic field configuration provided by 3D non-linear force-free field simulations of Mackay and van Ballegooijen (2009). The distributions of the temperature (including the PCTR) and the pressure of the plasma inserted into the magnetic dips are generated using the iterative hydrostatic method of Gunár et al. (2013). The synthetic images of the modelled prominence are produced using the Hα visualization method of Heinzel et al. (2015aa).

In Fig. 12, we highlight the changes in the morphology of the modelled prominence that might be misinterpreted as signs of a rotation. This time-series of snapshots shows the evolution of the modelled prominence due to changes in the underlying photospheric magnetic flux configuration. We focus here on the tilt of the brightest part of the simulated prominence (in this case the prominence barb) and on the angle between the estimated axis of the prominence barb (green dot-dashed lines) and the vertical (white dot-dashed lines). This angle is changing over time as the barb shifts its tilt from the left to the right. Such a change could suggest a seemingly rotational motion where the base of a tornado-like prominence is static while its top swirls around the vertical axis, as sketched in Fig. 12. However, from the 3D model, it is clear that there is no rotational motion of the modelled fine structures and the perceived tilt of the prominence is a consequence of a rearrangement of these fine structures caused by the changes in the underlying photospheric flux distribution. The seemingly rotational movement is thus only a consequence of the natural propensity of our brains to associate what we momentarily see with what we already know.

6.4 Seemingly Circular Traces of Magnetic Field Lines as a Consequence of Projection Effects

'Prominence tornadoes' that exhibit seemingly cyclonic motions of fine structures around their horizontal axis parallel to the line of sight (Li et al. 2012, variety) can be also explained by non-rotational movements of prominence plasma along predominantly horizontal field lines. Such a scenario, which is consistent with the observational findings of Schmieder et al. (2017b), was discussed by Gunár et al. (2018). Using the 3D WPFS model, these authors demonstrated that when the naturally three-dimensional prominences are projected onto a two-dimensional plane-of-the-sky at certain viewing angles the traces of dipped magnetic field lines may exhibit circular or elliptical shapes. This is demonstrated in Fig. 13, where we plot dipped portions of the magnetic field lines of the 3D WPFS model in three orthogonal projections–onto the horizontal x-y plane (filament view) and the vertical planes x-z and

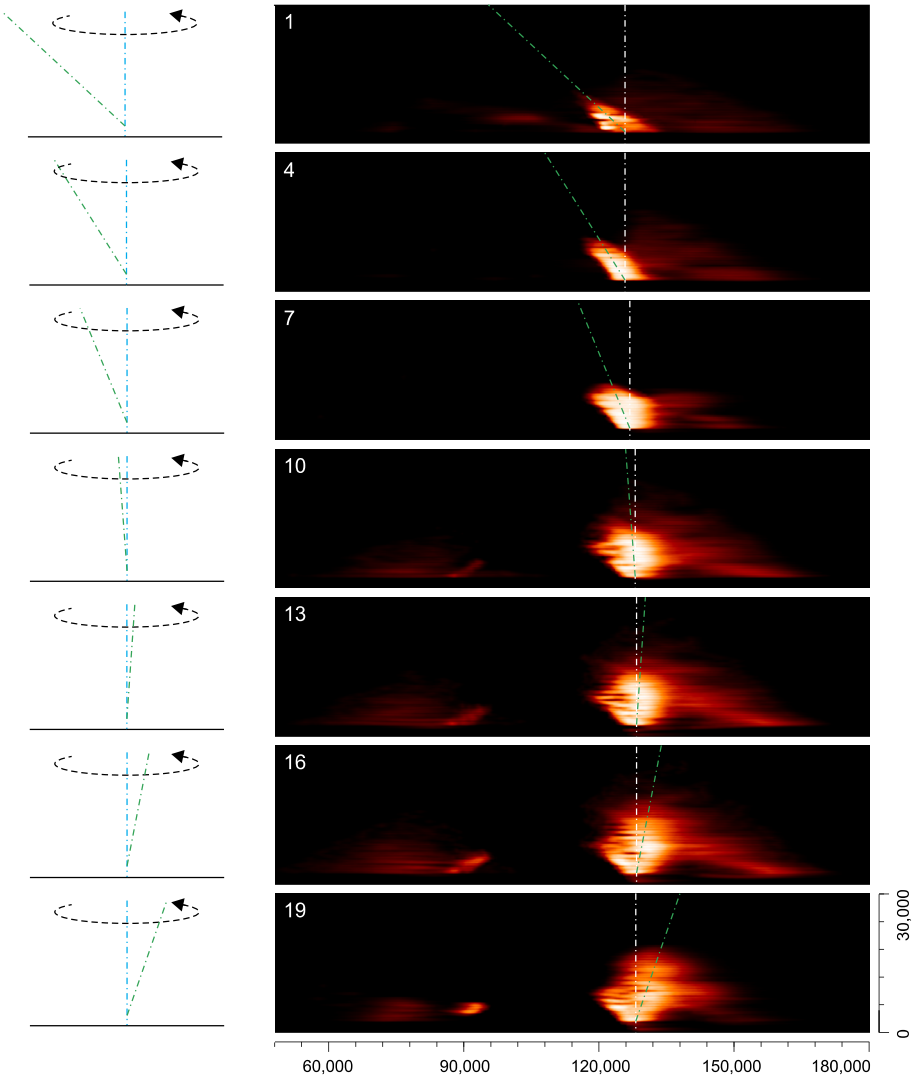

Fig. 12 An evolution of a prominence shown as a time-series of synthetic Hα snapshots produced by the 3D WPFS model of Gunár and Mackay (2015a,b). The green dot-dashed lines highlight the estimated axis of the brightest part of the prominence in individual snapshots and the white dot-dashed lines denote the vertical. Sketches on the left depict a scenario in which the tilted axis of the prominence swirls around the vertical. Dimensions are given in km. This figure is adapted from Fig. 1 of Gunár and Mackay (2015b)

y-z (prominence views). In the projection onto the y-z plane (see its zoomed-in part) it is clearly visible that the highlighted field lines have circular/elliptical shape. This means that any prominence fine structure movement that would happen along such field lines would in this projection appear as a rotational motion similar to that reported by Li et al. (2012). However, from the projection onto the x-z plane it is obvious that the highlighted field lines are in fact slightly dipped but dominated by the horizontal component of the field. Therefore,

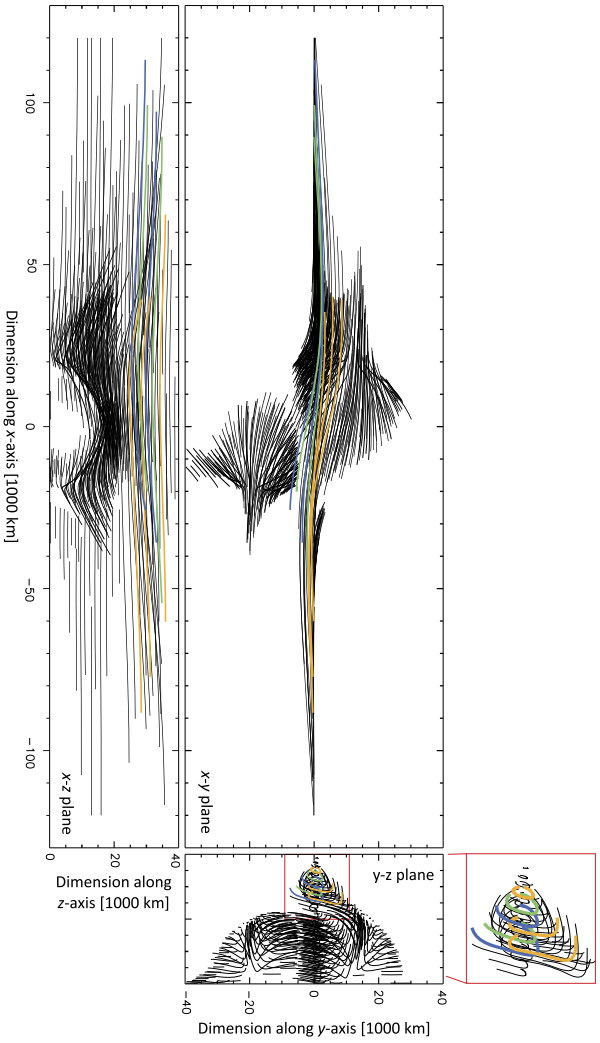

Fig. 13 Entire dipped parts of the field lines of the 3D WPFS model of Gunár et al. (2018) are plotted in three orthogonal projections–onto the x-y, x-z and y-z planes. The same selected field lines are highlighted with colors in all three projections. Dimensions are in units of 1,000 km. This figure is adapted from Fig. 8 of Gunár et al. (2018)

any movement of fine structures along these field lines would in fact be predominantly horizontal.

7 Summary

The term 'tornado' was used in recent years to describe various solar phenomena, ranging from large-scale eruptive prominences to small-scale photospheric vortices. The swirling fine-structure motions visible during prominence eruptions, which may be evocative of the name 'tornado' are generally accepted to be the manifestations of the unwinding of the twisted prominence magnetic field configurations during the eruption. As such, these rotational motions are neither coherent nor sustained for long periods. Therefore, in our opinion, they do not warrant the name of the terrestrial phenomena, and are not the subject of this

work. Neither are the small-scale photospheric and chromospheric vortex flows that are short-lived but seem to be abundant in the lower solar atmosphere, and can be identified down to the resolution limit of the current instrument and simulations. As such, these vortices are not directly associated with prominences, as we make clear in their description in Sect. 2. In this paper, we focus on the generally stable quiescent prominences, some of which were named 'tornadoes' by Pettit (see Sect. 3 for a detailed historical overview). This name was recently re-applied to prominences, starting a renewed interest in this fascinating topic – see Sect. 4.

Even in the case of quiescent prominences, 'tornado' is used as a name for two distinct configurations observed above the solar limb: vertical column-like structures (e.g., Su et al. 2012; Wedemeyer et al. 2013a), and horizontal cylindrical structures viewed along their axis (e.g. Li et al. 2012). In the first case, the notion of rotation around the vertical axis of the column-like prominences comes from the Doppler-shift patterns derived from spectroscopic measurements. In the second case, helical motions of fine structures along the horizontal axis parallel to the line of sight seem to be apparent from high-cadence imaging observations. However, as we demonstrate in this work, there is ample observational (Sect. 5) and theoretical (Sect. 6) evidence which strongly suggests that none of the so-called 'prominence tornadoes' are rotating in a sustained and coherent manner.

Let us first focus on the horizontal 'tornadoes' of Li et al. (2012) variety. In these prominences, which we observe along their horizontal axis, several authors identified movements of fine structures following helical trajectories. Such cyclonic dynamics may loosely evoke the image of terrestrial tornadoes, albeit horizontal ones. However, reconstructions of the true 3D trajectories of such moving prominence fine structures (see Sect. 5.2) show that the perceived rotational movements are likely a consequence of the projection into the plane-of-the-sky. The dominant part of the velocity vector of the reconstructed trajectories of the observed prominence fine structures is typically horizontal (Schmieder et al. 2017). This is further corroborated by the theoretical 3D modelling of Gunár et al. (2018) discussed in Sect. 6.4. These authors showed that traces of otherwise predominantly horizontal magnetic field lines can in certain projections appear distinctly helical. Perspective and the projection effects thus play a large role in the visual impression of rotation in these prominences.

When we look at the column-like prominences of Su et al. (2012) and Wedemeyer et al. (2013a) variety, there are two main characteristics that evoke the name 'tornado'. The first is the shape of the silhouettes of prominences visible especially in the AIA 171 Å and 193 Å channels. These silhouettes appear as slim vertical columns, sometimes with a funnel-like top. However, while these suggestive shapes are visible in some wavelengths, they are not present in others (notably in the optically thick channels such as 304 Å), even in the case of the same observed prominences. Moreover, Su et al. (2012) or Wedemeyer et al. (2013a) found a clear correspondence between the dark columns of prominences and the barbs (or legs) of filaments observed on the solar disk. This suggests that filament barbs may at certain wavelengths and at certain projection angles appear as isolated funnel-like structures.

Furthermore, there are no direct measurements of rotation in the imaging observations of the column-like prominences. The notion of rotation comes from split red-and-blue Doppler-shift patterns, or is inferred from the presence of nearby photospheric vortices (observed on the disk several days prior to the prominence observations) or the swirling fine-structure motions when prominences eventually erupt. The split Doppler-shift patterns, where one side of the vertical prominence shows 'red' and the other side 'blue' LOS velocities are thus the second aspect evoking the name 'tornado'. Such patterns could be taken as a sign of rotation of entire column-like structures around their vertical axis, if sustained for long periods of time and unequivocally proven not to be caused by instrumental artefacts – see the discussion of the instrumental effects caused by the chromatic PSF of Hinode/EIS in Sect. 5.1.1.

However, such an explanation is only one of the possible scenarios leading to the split red-and-blue Doppler-shift patterns. Especially in the case when the column-like appearance is just a projection of slab-like prominence barbs, similar patterns can arise from an expansion (or contraction) of the entire prominence. In and even more likely scenario, prominence fine structure oscillations or the presence of counter-streaming flows can also lead to the split red-and-blue Doppler-shift patterns, as we also discuss in Sect. 6.2. These are, however, continually changing and resemble rotation of entire prominences only occasionally and by coincidence. For example, Martínez González et al. (2016) or Kucera et al. (2018) concluded that if the signs of rotation exist in the complex environment of the dynamic prominence fine structures, they are intermittent. However, the observed Doppler-shift patterns are more consistent with either the motions of discrete structures making up the barb or with oscillations. Therefore, the coincidental and localised signatures of the perceived rotation cannot be taken as an unequivocal sign of a sustained rotation of entire prominence structures.

This is further corroborated by the measurements of the prominence magnetic field that generally confirm the presence of horizontal fields – see Sect. 5.3. Only some prominence magnetic field measurements seem to support the idea of helical magnetic field structure spiralling along the vertical axis of prominences. However, due to the inherent ambiguities of the magnetic field inference, these results rely on rather strong assumptions.

8 Conclusions

This careful review of the publications presenting the recent observational data and theoretical models leads us to conclude that there are no sustained and coherent rotational movements in the prominence structures referred to as 'tornadoes'. The visual impression of helical movements of prominence fine structures and the measured split red-and-blue Doppler-shift patterns can easily be explained by projection effects and the presence of oscillations and/or counter-streaming flows. This conclusion also respects the overwhelming number of measurements of horizontal prominence magnetic fields and confirms the magnetic topology that has been demonstrated to be able to support the dense prominence plasma in a stable manner. 'Prominence tornados' thus do not differ in any substantial way from other solar prominences. In fact, they are manifestations of the same complex solar phenomena, just observed in two specific projections. These significantly different views of the same phenomena, compounded by the presence of dynamics and simple yet profoundly distorting projection effects may sometimes play havoc with our intuitive understanding of perceived shapes and movements, understanding that was trained by evolution on solid objects that surround us. Therefore, there is no need for the distinct category of 'tornado' prominences.

More so, there is no need for the term 'tornado' when referring to prominences. This is because, when the name is used, it brings to mind the atmospheric column-like vortices of very fast sustained speeds that propagate downwards from large rotating clouds. Terrestrial tornadoes appear dark in the contrast to the bright daylight sky and surrounding clouds but the air in them is not significantly heavier than that in the tornado vicinity. The opacity of the atmospheric tornadoes is caused by the presence of dust, moisture, and debris. And, of course, there is no magnetic field to consider. These are characteristics that are unlike those of solar prominences, where the rotation is intermittent (if present at all) and the dense prominence material must be supported against the gravity. Therefore, the use of the name 'tornado' when referring to prominences may cause us to search for evidence supporting our

mental image of atmospheric tornadoes where no such evidence is present. To justify the analogy with terrestrial tornadoes we would need to find prominences exhibiting coherent and fast rotational motions for their entire lifetimes. Only in such a case the term 'tornado' will not lead to confusion and unnecessary over-interpretation of observations.

Of course, the available observational data are still limited. One of the most critical limiting factors is the fact that, apart from instances when, thanks to STEREO (Solar TErrestrial RElations Observatory; Kaiser et al. 2008) spacecraft, we could observe the same prominences from several different angles (see, e.g., Bemporad 2011), we had to rely only on a single viewing angle at a time. However, as the present paper demonstrates, the role of the perspective and projection effects in understanding of the nature of prominences is crucial.

Therefore, to further confirm the conclusions of this work, we will take advantage of the capabilities of Solar Orbiter (Müller et al. 2020) to provide multi-angle observations of prominences/filaments. In the future, such multi line-of-sight observations will be greatly enhanced by the planned mission at L5. Ideally, having simultaneous observations from three vantage points – Earth/L1/SDO, L5, and Solar Orbiter when observing from out of the ecliptic – would provide the ultimate test as to whether prominence tornadoes exist or not.

Appendix A: Dark Prominence Features in the SDO/AIA Coronal Channels

It may seem counter-intuitive that we can observe the cool plasma of prominences in the hot coronal channels of SDO/AIA and other EUV imagers, such as Extreme-Ultraviolet Imaging Telescope (EIT; Delaboudinière et al. 1995) onboard the Solar and Heliospheric Observatory (SOHO) or the Extreme Ultraviolet Imager (EUI; Rochus et al. 2020) onboard Solar Orbiter. The EUV coronal emission visible in the AIA 171 Å and 193 Å channels is formed at temperatures around and above 1 MK while the cool plasma constituting the cores of prominence fine structures is below 10,000 K. However, the cool prominence material present in the corona attenuates the coronal EUV radiation by two mechanisms: absorption and emissivity blocking.

In the first case, the reduction of the observed coronal brightness stems from the fact that the radiation of all EUV lines with wavelengths below the head of the hydrogen Lyman continuum at 912 Å can be absorbed by neutral hydrogen, which is abundant in cool prominence structures (Schmahl and Orrall 1979). For even shorter wavelengths additional absorption by neutral helium can occur (below 504 Å), and for very short wavelengths (below 228 Å) singly ionised helium will also contribute under specific conditions. As was described in detail by, e.g., Anzer and Heinzel (2005), this absorption is the photoionization of H I, He I, and He II atoms by the coronal EUV radiation. As these authors showed, in prominences the optical thickness of the resonance continua of H I, He I, and He II at the wavelengths covered by the 171 Å or 193 Å channels of AIA is comparable to the optical thickness of the Hα line.

The secondary contributing mechanism is called emissivity blocking, also known as volume blocking in, e.g. Anzer and Heinzel (2005). The emissivity-blocking effect occurs because the prominence material present in the corona does not emit any EUV radiation from the volume occupied by the cool plasma, while the surrounding corona emits from its entire volume. This causes an additional reduction of the intensity emanating from the location of the observed prominence compared to the surrounding corona.

These two mechanisms together reduce the background coronal radiation enough to reveal the structure of prominences as dark silhouettes against the bright coronal background (see, e.g., Kucera et al. 1998; Schmieder et al. 2004, for more details).

Appendix B: Optically Thick and Optically Thin Diagnostics of Spectral-Line Doppler Shifts

In this appendix we first describe the general use of the LOS velocity diagnostics using the Doppler shifts of optically thick and optically thin spectral lines. In the later part we focus on the properties of the spectral lines observed by IRIS. It is important to remember that velocities derived from Doppler shifts do not always provide true information about the LOS component of the velocity of the observed plasma structures. This is caused by several factors, from which the most important is the optical thickness of the observed plasma in the observed spectral line.

B.1 Optically Thick Case

In the optically very thick case, the observed spectral line is produced in a narrow region closest to the observer (with a caveat we will describe later). This means that the Doppler shift of such a spectral line provides information about the true LOS velocity of that particular region. However, we do not gain any insight into the movement of the plasma beyond this region unless the spectral line in question is narrow and thus very sensitive to the velocity. Then we can obtain complex profiles with a contribution from deeper regions. This was demonstrated for example by Heinzel et al. (2014, 2015bb) who showed that the complex, multi-peak Mg II h&k profiles (see Fig. 14) observed in prominences by IRIS can be explained by the presence of different plasma structures moving with different LOS velocities. Multi-peaked Mg II h&k profiles were also produced by Tei et al. (2020) and Gunár et al. (2022) using multi-thread models with stochastic LOS dynamics. We note that the decreased intensity of the side peaks (Fig. 14) can be explained by the Doppler dimming effect in the Mg II h&k lines described for example by Heinzel et al. (2015bb). While we do not focus on the Doppler dimming/brightening effect here, we note that this effect may also influence the Doppler-shift analysis of the LOS velocities by modifying the complexity of the line profile asymmetries.

We should now ask why we can obtain information from the plasma located beyond the first plasma structure even in optically very thick case? This is due to the fact that the observed plasma is optically very thick only near the centre of a spectral line. The optical thickness decreases away from the line centre to values well below unity in far wings. Therefore, in the wings of optically thick spectral lines we can 'see beyond' the first structure in which the centre of the line is formed. If the difference between the LOS velocities

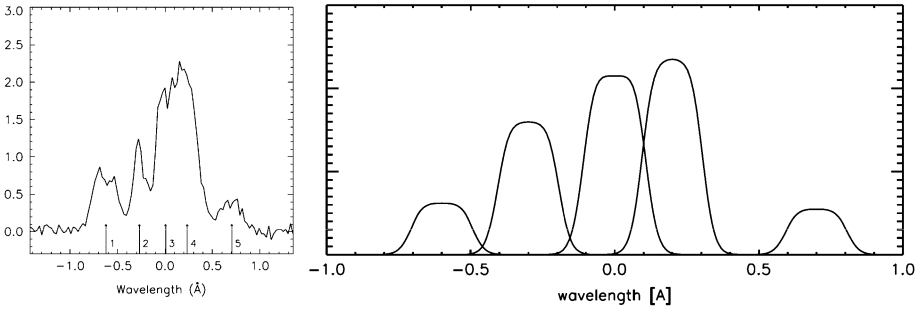

Fig. 14 Left: An example of observed multi-peaked Mg II k profile obtained by IRIS (adapted from Schmieder et al. 2014b). Right: Simulated multi-peaked Mg II k profile (adapted from Heinzel et al. 2015bb)

of individual plasma structures causes a Doppler shift comparable or larger than the FWHM (Full Width at Half-Maximum) of the considered spectral line in a single structure, then we can easily identify individual components of complex, multi-peak observed profiles, such as in the case of Heinzel et al. (2015bb, Fig. 1) or Ruan et al. (2018, Fig. 14). On the other hand, if the difference between the LOS velocities of these plasma structures is significantly smaller than the FWHM of a single structure, the resulting spectral line profile will appear strongly asymmetric or reversed. The LOS velocity derived from the Doppler shift of an entire line profile in such a case does not convey information about the absolute LOS velocity of the nearest, or any other individual plasma structure, but of a superposition of all of them. Therefore, if such an asymmetric profile is analysed in the context of a single moving plasma structure, the obtained Doppler-shift velocity does not provide a truly accurate measurement. The difference between the true LOS velocities of individual plasma structures and the apparent Doppler-shift velocity derived from their superposition may be significant.

The described analysis of the optically thick spectral lines is further complicated by the fact that such spectral lines, for example Mg II h&k or hydrogen Lyman lines, are often naturally reversed due to the behaviour of their source functions. This means that it may be impossible to distinguish between a two-component spectral line formed when two independent plasma structures move with different LOS velocities and a single-component but naturally reversed spectral line from a single plasma structure. An example may be found in Gunár et al. (2008), where the authors studied asymmetries of hydrogen Lyman line profiles caused by movement of multiple prominence plasma structures with stochastic LOS velocities. These authors showed that the strong and sometimes even opposite asymmetries in different Lyman lines can be caused by realistic, relatively low stochastic LOS velocities of individual fine structures and not by several times larger LOS velocity of a supposedly uniform plasma structure. However, we note that it might be possible to distinguish between multi-component and single-component cases when two (or more) spectral lines are analysed together. An example of such a pair of spectral lines are Mg II h&k and C II lines observed by IRIS.

B.2 Optically Thin Case

In the optically thin case the information about the LOS movement of all plasma structures propagates through the entire observed medium and is integrated into the final spectral line profile. This means that the resulting profile contains a superposition of Doppler shifts from all individual plasma structures. If these structures again move with sufficiently different LOS velocities (producing Doppler shifts comparable or larger than the FWHM of a single structure) we will observe clearly separated individual spectral line components. We are then able to derive the true LOS velocities of individual plasma structures. However, if these structures move with LOS velocities which do not cause sufficiently large Doppler shifts, the resulting profile will be broadened and generally asymmetric. Moreover, we can imagine a simple scenario in which two "identical" plasma structures move with equal but opposite LOS velocities. In such a case, the resulting spectral profile might be even symmetric and centred around the zero (rest) wavelength. This means that we would not measure any Doppler shift and thus assume that we observe a single, stationary plasma structure while we are observing two structures with potentially significant LOS velocities. Such scenario was discussed for example by Gunár et al. (2012). Of course, in reality the situation in observations is even more complex. This simple example just illustrates that information about the LOS velocities derived from Doppler shifts is not always robust.

From the differences between optically thin and thick cases it is clear that in many circumstances we will obtain different LOS velocities derived from Doppler shifts when different optically thick and optically thin spectral lines are used. This is illustrated for example by the work of Ruan et al. (2018), which shows that the LOS velocities derived from Doppler shifts of the Mg II h&k profiles observed by IRIS can be different (often larger) than those derived from the Hα observations. This again demonstrates that the LOS velocity diagnostics employing the analysis of the spectral-line Doppler shifts need to be approached with caution and only detailed radiative-transfer simulations can help to distinguish various situations.

Acknowledgements This paper stemmed from the discussions held at ISSI during two meetings of the International Team 374 ("Solving the prominence paradox", led by N. Labrosse) in February 2017 and March 2018. We acknowledge fruitful discussions with all who participated in these meetings including L. Green, S. Gunár, P. Heinzel, S. Jejčič, J.M. Jenkins, T.A. Kucera, N. Labrosse, P.J. Levens, A. López Ariste, M. Luna, D.H. Mackay, O. Panasenco, T. Rees-Crockford, A. Rodger, T. Roudier, B. Schmieder, S. Wedemeyer, and M. Zapiór.

We thank I. Ugarte-Urra for providing the Hinode/EIS deconvolution routine used in Warren et al. (2018). Hinode is a Japanese mission developed and launched by ISAS/JAXA, with NAOJ as domestic partner and NASA and STFC (UK) as international partners. It is operated by these agencies in cooperation with ESA and NSC (Norway).

Author Contribution Petr Heinzel, Therese A. Kucera, Peter J. Levens, Arturo López Ariste, Duncan H. Mackay, Maciej Zapiór contributed equally to this work.

Funding Open access publishing supported by the National Technical Library in Prague. S. Gunár and P. Heinzel acknowledge the support from grant 22-34841S of the Czech Science Foundation (GAČR). S. Gunár, P. Heinzel, and M. Zapiór acknowledge the support from the project RVO:67985815 of the Astronomical Institute of the Czech Academy of Sciences. N. Labrosse acknowledges support from STFC grant ST/T000422/1. M. Luna acknowledges support through the Ramón y Cajal fellowship RYC2018-026129-I from the Spanish Ministry of Science and Innovation, the Spanish National Research Agency (Agencia Estatal de Investigación), the European Social Fund through Operational Program FSE 2014 of Employment, Education and Training and the Universitat de les Illes Balears. This publication is part of the R + D + i project PID2020-112791GB-I00, financed by MCIN/AEI/10.13039/501100011033. T. Kucera acknowledges support of the NASA Heliophysics ISFM program. D.H.M. would like to thank the STFC for support via consolidated grant ST/W001195/1.

Declarations

Competing Interests The authors are not aware of any conflicts of interest (financial or otherwise) in connection with the presented work.

References

Antolin P, Okamoto TJ, De Pontieu B, Uitenbroek H, Van Doorsselaere T, Yokoyama T (2015) Resonant absorption of transverse oscillations and associated heating in a solar prominence. II. Numerical aspects. Astrophys J 809:72. https://doi.org/10.1088/0004-637X/809/1/72. arXiv:1506.09108 [astro-ph.SR]

Anzer U, Heinzel P (2005) On the nature of dark extreme ultraviolet structures seen by SOHO/EIT and TRACE. Astrophys J 622(1):714–721. https://doi.org/10.1086/427817

Arregui I, Oliver R, Ballester JL (2018) Prominence oscillations. Living Rev Sol Phys 15(1):3

Aulanier G, Démoulin P (1998) 3-D magnetic configurations supporting prominences. I. The natural presence of lateral feet. Astron Astrophys 329:1125–1137

Barczynski K, Schmieder B, Peat AW, Labrosse N, Mein P, Mein N (2021) Spectro-imagery of an active tornado-like prominence: formation and evolution. Astron Astrophys 653:A94. https://doi.org/10.1051/0004-6361/202140976. arXiv:2106.04259 [astro-ph.SR]

Bemporad A (2011) Prominence 3D reconstruction in the STEREO era: a review. J Atmos Sol-Terr Phys 73(10):1117–1128. https://doi.org/10.1016/j.jastp.2010.12.007

Berger TE, Shine RA, Slater GL, Tarbell TD, Title AM, Okamoto TJ, Ichimoto K, Katsukawa Y, Suematsu Y, Tsuneta S, Lites BW, Shimizu T (2008) Hinode SOT observations of solar quiescent prominence dynamics. Astrophys J Lett 676:L89–L92. https://doi.org/10.1086/587171

Bonet JA, Márquez I, Sánchez Almeida J, Cabello I, Domingo V (2008) Convectively driven vortex flows in the sun. Astrophys J Lett 687(2):L131. https://doi.org/10.1086/593329. arXiv:0809.3885 [astro-ph]

Casini R, Bevilacqua R, López Ariste A (2005) Principal component analysis of the He I D_3 polarization profiles from solar prominences. Astrophys J 622(2):1265–1274. https://doi.org/10.1086/428283

Casini R, López Ariste A, Paletou F, Léger L (2009) Multi-line Stokes inversion for prominence magnetic-field diagnostics. Astrophys J 703(1):114–120. https://doi.org/10.1088/0004-637X/703/1/114. arXiv:0906.2144 [astro-ph.IM]

Chae J (2010) Dynamics of vertical threads and descending knots in a hedgerow prominence. Astrophys J 714:618–629. https://doi.org/10.1088/0004-637X/714/1/618

Chae J, Moon YJ, Park YD (2005) The magnetic structure of filament barbs. Astrophys J 626:574–578. https://doi.org/10.1086/429797

Chen H, Zhang J, Ma S, Yan X, Xue J (2017) May. solar tornadoes triggered by interaction between filaments and EUV jets. Astrophys J Lett 841(1):L13. https://doi.org/10.3847/2041-8213/aa71a2

Chen H, Zhang J, De Pontieu B, Ma S, Kliem B, Priest E (2020) Coronal mini-jets in an activated solar tornado-like prominence. Astrophys J 899(1):19. https://doi.org/10.3847/1538-4357/ab9cad. arXiv:2006.08252 [astro-ph.SR]

Culhane JL, Harra LK, James AM, Al-Janabi K, Bradley LJ, Chaudry RA, Rees K, Tandy JA, Thomas P, Whillock MCR, Winter B, Doschek GA, Korendyke CM, Brown CM, Myers S, Mariska J, Seely J, Lang J, Kent BJ, Shaughnessy BM, Young PR, Simnett GM, Castelli CM, Mahmoud S, Mapson-Menard H, Probyn BJ, Thomas RJ, Davila J, Dere K, Windt D, Shea J, Hagood R, Moye R, Hara H, Watanabe T, Matsuzaki K, Kosugi T, Hansteen V, Wikstol Ø (2007) The EUV imaging spectrometer for hinode. Sol Phys 243:19–61. https://doi.org/10.1007/s01007-007-0293-1

De Pontieu B, Title AM, Lemen JR, Kushner GD, Akin DJ, Allard B, Berger T, Boerner P, Cheung M, Chou C, Drake JF, Duncan DW, Freeland S, Heyman GF, Hoffman C, Hurlburt NE, Lindgren RW, Mathur D, Rehse R, Sabolish D, Seguin R, Schrijver CJ, Tarbell TD, Wülser JP, Wolfson CJ, Yanari C, Mudge J, Nguyen-Phuc N, Timmons R, van Bezooijen R, Weingrod I, Brookner R, Butcher G, Dougherty B, Eder J, Knagenhjelm V, Larsen S, Mansir D, Phan L, Boyle P, Cheimets PN, DeLuca EE, Golub L, Gates R, Hertz E, McKillop S, Park S, Perry T, Podgorski WA, Reeves K, Saar S, Testa P, Tian H, Weber M, Dunn C, Eccles S, Jaeggli SA, Kankelborg CC, Mashburn K, Pust N, Springer L, Carvalho R, Kleint L, Marmie J, Mazmanian E, Pereira TMD, Sawyer S, Strong J, Worden SP, Carlsson M, Hansteen VH, Leenaarts J, Wiesmann M, Aloise J, Chu KC, Bush RI, Scherrer PH, Brekke P, Martinez-Sykora J, Lites BW, McIntosh SW, Uitenbroek H, Okamoto TJ, Gummin MA, Auker G, Jerram P, Pool P, Waltham N (2014) The Interface Region Imaging Spectrograph (IRIS). Sol Phys 289:2733–2779

Delaboudinière JP, Artzner GE, Brunaud J, Gabriel AH, Hochedez JF, Millier F, Song XY, Au B, Dere KP, Howard RA, Kreplin R, Michels DJ, Moses JD, Defise JM, Jamar C, Rochus P, Chauvineau JP, Marioge JP, Catura RC, Lemen JR, Shing L, Stern RA, Gurman JB, Neupert WM, Maucherat A, Clette F, Cugnon P, van Dessel EL (1995) EIT: extreme-ultraviolet imaging telescope for the SOHO mission. Sol Phys 162:291–312. https://doi.org/10.1007/BF00733432

Dudík J, Aulanier G, Schmieder B, Bommier V, Roudier T (2008) Topological departures from translational invariance along a filament observed by THEMIS. Sol Phys 248:29–50. https://doi.org/10.1007/s11207-008-9155-2

Gibson S (2015) Coronal cavities: observations and implications for the magnetic environment of prominences. In: Vial J-C, Engvold O (eds) Solar prominences. Astrophysics and space science library, vol 415, p 323

Gibson SE (2018) Solar prominences: theory and models. Fleshing out the magnetic skeleton. Living Rev Sol Phys 15(1):7. https://doi.org/10.1007/s41116-018-0016-2

Gilbert HR, Hansteen VH, Holzer TE (2002) Neutral atom diffusion in a partially ionized prominence plasma. Astrophys J 577(1):464–474. https://doi.org/10.1086/342165

Gilbert H, Kilper G, Alexander D (2007) Observational evidence supporting cross-field diffusion of neutral material in solar filaments. Astrophys J 671(1):978–989. https://doi.org/10.1086/522884

Gunár S, Mackay DH (2015a) 3D whole-prominence fine structure modeling. Astrophys J 803:64. https://doi.org/10.1088/0004-637X/803/2/64

Gunár S, Mackay DH (2015b) 3D whole-prominence fine structure modeling. II. Prominence evolution. Astrophys J 812:93. https://doi.org/10.1088/0004-637X/812/2/93

Gunár S, Heinzel P, Anzer U, Schmieder B (2008) On Lyman-line asymmetries in quiescent prominences. Astron Astrophys 490:307–313. https://doi.org/10.1051/0004-6361:200810127

Gunár S, Schwartz P, Schmieder B, Heinzel P, Anzer U (2010) Statistical comparison of the observed and synthetic hydrogen Lyman line profiles in solar prominences. Astron Astrophys 514:A43. https://doi.org/10.1051/0004-6361/200913411

Gunár S, Mein P, Schmieder B, Heinzel P, Mein N (2012) Dynamics of quiescent prominence fine structures analyzed by 2D non-LTE modelling of the Hα line. Astron Astrophys 543:A93. https://doi.org/10.1051/0004-6361/201218940

Gunár S, Mackay DH, Anzer U, Heinzel P (2013) Non-linear force-free magnetic dip models of quiescent prominence fine structures. Astron Astrophys 551:A3. https://doi.org/10.1051/0004-6361/201220597

Gunár S, Dudík J, Aulanier G, Schmieder B, Heinzel P (2018) Importance of the Hα visibility and projection effects for the interpretation of prominence fine-structure observations. Astrophys J 867:115. https://doi.org/10.3847/1538-4357/aae4e1

Gunár S, Heinzel P, Koza J, Schwartz P (2022) Large impact of the Mg II h and k incident radiation change on results of radiative transfer models and the importance of dynamics. Astrophys J 934(2):133. https://doi.org/10.3847/1538-4357/ac7397

Handy BN, Acton LW, Kankelborg CC, Wolfson CJ, Akin DJ, Bruner ME, Caravalho R, Catura RC, Chevalier R, Duncan DW, Edwards CG, Feinstein CN, Freeland SL, Friedlaender FM, Hoffmann CH, Hurlburt NE, Jurcevich BK, Katz NL, Kelly GA, Lemen JR, Levay M, Lindgren RW, Mathur DP, Meyer SB, Morrison SJ, Morrison MD, Nightingale RW, Pope TP, Rehse RA, Schrijver CJ, Shine RA, Shing L, Strong KT, Tarbell TD, Title AM, Torgerson DD, Golub L, Bookbinder JA, Caldwell D, Cheimets PN, Davis WN, Deluca EE, McMullen RA, Warren HP, Amato D, Fisher R, Maldonado H, Parkinson C (1999) The transition region and coronal explorer. Sol Phys 187(2):229–260. https://doi.org/10.1023/A:1005166902804

Heinzel P, Vial JC, Anzer U (2014) On the formation of Mg ii h and k lines in solar prominences. Astron Astrophys 564:A132. https://doi.org/10.1051/0004-6361/201322886

Heinzel P, Gunár S, Anzer U (2015a) Fast approximate radiative transfer method for visualizing the fine structure of prominences in the hydrogen Hα line. Astron Astrophys 579:A16. https://doi.org/10.1051/0004-6361/201525716

Heinzel P, Schmieder B, Mein N, Gunár S (2015b) Understanding the Mg II and Hα spectra in a highly dynamical solar prominence. Astrophys J 800:L13. https://doi.org/10.1088/2041-8205/800/1/L13

Jenkins JM, Keppens R (2022) Resolving the solar prominence/filament paradox using the magnetic Rayleigh-Taylor instability. Nat Astron. https://doi.org/10.1038/s41550-022-01705-z

Kaiser ML, Kucera TA, Davila JM, Cyr OCSt, Guhathakurta M, Christian E (2008) The STEREO mission: an introduction. Space Sci Rev 136(1–4):5–16. https://doi.org/10.1007/s11214-007-9277-0

Kosugi T, Matsuzaki K, Sakao T, Shimizu T, Sone Y, Tachikawa S, Hashimoto T, Minesugi K, Ohnishi A, Yamada T, Tsuneta S, Hara H, Ichimoto K, Suematsu Y, Shimojo M, Watanabe T, Shimada S, Davis JM, Hill LD, Owens JK, Title AM, Culhane JL, Harra LK, Doschek GA, Golub L (2007) The hinode (Solar-B) mission: an overview. Sol Phys 243:3–17. https://doi.org/10.1007/s11207-007-9014-6

Kucera TA, Andretta V, Poland AI (1998) Neutral hydrogen column depths in prominences using EUV absorption features. Sol Phys 183(1):107–121. https://doi.org/10.1023/A:1005077417572

Kucera TA, Ofman L, Tarbell TD (2018) Motions in prominence barbs observed on the solar limb. Astrophys J 859:121. https://doi.org/10.3847/1538-4357/aabe90

Kupryakov YA, Kotrc P, Kashapova LK (2019) On the role of preflares in tornado-type prominences. Astron Astrophys Trans 31(2):177–182

Labrosse N, Heinzel P, Vial J, Kucera T, Parenti S, Gunár S, Schmieder B, Kilper G (2010) Physics of solar prominences: I: spectral diagnostics and non-LTE modelling. Space Sci Rev 151:243–332. https://doi.org/10.1007/s11214-010-9630-6. arXiv:1001.1620 [astro-ph.SR]

Lemen JR, Title AM, Akin DJ, Boerner PF, Chou C, Drake JF, Duncan DW, Edwards CG, Friedlaender FM, Heyman GF, Hurlburt NE, Katz NL, Kushner GD, Levay M, Lindgren RW, Mathur DP, McFeaters EL, Mitchell S, Rehse RA, Schrijver CJ, Springer LA, Stern RA, Tarbell TD, Wuelser JP, Wolfson CJ, Yanari C, Bookbinder JA, Cheimets PN, Caldwell D, Deluca EE, Gates R, Golub L, Park S, Podgorski WA, Bush RI, Scherrer PH, Gummin MA, Smith P, Auker G, Jerram P, Pool P, Soufli R, Windt DL, Beardsley S, Clapp M, Lang J, Waltham N (2012) The Atmospheric Imaging Assembly (AIA) on the Solar Dynamics Observatory (SDO). Sol Phys 275:17–40. https://doi.org/10.1007/s11207-011-9776-8

Levens PJ (2018) Diagnostics of solar tornado-like prominences. Ph. D. thesis, University of Glasgow
Levens PJ, Labrosse N, Fletcher L, Schmieder B (2015) A solar tornado observed by EIS. Plasma diagnostics. Astron Astrophys 582:A27. https://doi.org/10.1051/0004-6361/201425586. arXiv:1508.01377 [astro-ph.SR]
Levens PJ, Schmieder B, Labrosse N, López Ariste A (2016) Structure of prominence legs: plasma and magnetic field. Astrophys J 818:31. https://doi.org/10.3847/0004-637X/818/1/31. arXiv:1512.04727 [astro-ph.SR]
Levens PJ, Schmieder B, López Ariste A, Labrosse N, Dalmasse K, Gelly B (2016) Magnetic field in atypical prominence structures: bubble, tornado, and eruption. Astrophys J 826:164. https://doi.org/10.3847/0004-637X/826/2/164. arXiv:1605.05964 [astro-ph.SR]
Levens PJ, Labrosse N, Schmieder B, López Ariste A, Fletcher L (2017) Comparing UV/EUV line parameters and magnetic field in a quiescent prominence with tornadoes. Astron Astrophys 607:A16. https://doi.org/10.1051/0004-6361/201730808. arXiv:1708.04606 [astro-ph.SR]
Li K, Zhong S (1997) The observations and analyses of an eruptive prominence. Astron Astrophys Suppl Ser 126:241–245. https://doi.org/10.1051/aas:1997261
Li X, Morgan H, Leonard D, Jeska L (2012) A solar tornado observed by AIA/SDO: rotational flow and evolution of magnetic helicity in a prominence and cavity. Astrophys J Lett 752:L22. https://doi.org/10.1088/2041-8205/752/2/L22. arXiv:1205.3819 [astro-ph.SR]
Liakh V, Luna M, Khomenko E (2020) Numerical simulations of large-amplitude oscillations in flux rope solar prominences. Astron Astrophys 637:A75. https://doi.org/10.1051/0004-6361/201937083. arXiv:2003.04343 [astro-ph.SR]
Liakh V, Luna M, Khomenko E (2021) Large-amplitude longitudinal oscillations in solar prominences simulated with different resolutions. Astron Astrophys 654:A145. https://doi.org/10.1051/0004-6361/202141524. arXiv:2108.01143 [astro-ph.SR]
Lin Y, Engvold OR, Wiik JE (2003) Counterstreaming in a large polar crown filament. Sol Phys 216:109–120. https://doi.org/10.1023/A:1026150809598
Lin Y, Engvold O, Rouppe van der Voort L, Wiik JE, Berger TE (2005) Thin threads of solar filaments. Sol Phys 226:239–254. https://doi.org/10.1007/s11207-005-6876-3
Lin Y, Martin SF, Engvold O, Rouppe van der Voort LHM, van Noort M (2008) On small active region filaments, fibrils and surges. Adv Space Res 42:803–811. https://doi.org/10.1016/j.asr.2007.05.052
López Ariste A, Casini R (2005) Inference of the magnetic field in spicules from spectropolarimetry of He I D3. Astron Astrophys 436(1):325–331. https://doi.org/10.1051/0004-6361:20042214
López Ariste A, Aulanier G, Schmieder B, Sainz Dalda A (2006) First observation of bald patches in a filament channel and at a barb endpoint. Astron Astrophys 456(2):725–735. https://doi.org/10.1051/0004-6361:20064923
Luna M, Díaz AJ, Karpen J (2012) The effects of magnetic-field geometry on longitudinal oscillations of solar prominences. Astrophys J 757(1):98
Luna M, Karpen JT, DeVore CR (2012) Formation and evolution of a multi-threaded solar prominence. Astrophys J 746:30. https://doi.org/10.1088/0004-637X/746/1/30. arXiv:1201.3559 [astro-ph.SR]
Luna M, Moreno-Insertis F, Priest E (2015) Are tornado-like magnetic structures able to support solar prominence plasma? Astrophys J 808(1):L23
Luna M, Terradas J, Khomenko E, Collados M, Vicente Ad (2016) On the robustness of the pendulum model for large-amplitude longitudinal oscillations in prominences. Astrophys J 817(2):157
Luna M, Karpen J, Ballester JL, Muglach K, Terradas J, Kucera T, Gilbert H (2018) GONG catalog of solar filament oscillations near solar maximum. Astrophys J Suppl Ser 236(2):35. https://doi.org/10.3847/1538-4365/aabde7. arXiv:1804.03743 [astro-ph.SR]
Luna M, Priest E, Moreno-Insertis F (2018) Self-similar approach for rotating magnetohydrodynamic solar and astrophysical structures. Astrophys J 863(2):147
Mackay DH, van Ballegooijen AA (2009) A non-linear force-free field model for the evolving magnetic structure of solar filaments. Sol Phys 260:321–346. https://doi.org/10.1007/s11207-009-9468-9
Mackay DH, Karpen JT, Ballester JL, Schmieder B, Aulanier G (2010) Physics of solar prominences: II magnetic structure and dynamics. Space Sci Rev 151:333–399. https://doi.org/10.1007/s11214-010-9628-0. arXiv:1001.1635 [astro-ph.SR]
Martínez González MJ, Manso Sainz R, Asensio Ramos A, Beck C, de la Cruz Rodríguez J, Díaz AJ (2015) Spectro-polarimetric imaging reveals helical magnetic fields in solar prominence feet. Astrophys J 802(1):3. https://doi.org/10.1088/0004-637X/802/1/3. arXiv:1501.03295 [astro-ph.SR]
Martínez González MJ, Asensio Ramos A, Arregui I, Collados M, Beck C, de la Cruz Rodríguez J (2016) On the magnetism and dynamics of prominence legs hosting tornadoes. Astrophys J 825:119. https://doi.org/10.3847/0004-637X/825/2/119. arXiv:1605.01183 [astro-ph.SR]
Mein P (1991) Solar 2D spectroscopy - a new MSDP instrument. Astron Astrophys 248:669–676

Mghebrishvili I, Zaqarashvili TV, Kukhianidze V, Ramishvili G, Shergelashvili B, Veronig A, Poedts S (2015) Dynamics of a solar prominence tornado observed by SDO/AIA on 2012 November 7-8. Astrophys J 810:89. https://doi.org/10.1088/0004-637X/810/2/89. arXiv:1508.06788 [astro-ph.SR]

Mghebrishvili I, Zaqarashvili TV, Kukhianidze V, Kuridze D, Tsiklauri D, Shergelashvili BM, Poedts S (2018) Association between tornadoes and instability of hosting prominences. Astrophys J 861(2):112. https://doi.org/10.3847/1538-4357/aac823. arXiv:1807.01345 [astro-ph.SR]

Müller D, Cyr OCSt, Zouganelis I, Gilbert HR, Marsden R, Nieves-Chinchilla T, Antonucci E, Auchère F, Berghmans D, Horbury TS, Howard RA, Krucker S, Maksimovic M, Owen CJ, Rochus P, Rodriguez-Pacheco J, Romoli M, Solanki SK, Bruno R, Carlsson M, Fludra A, Harra L, Hassler DM, Livi S, Louarn P, Peter H, Schühle U, Teriaca L, del Toro Iniesta JC, Wimmer-Schweingruber RF, Marsch E, Velli M, De Groof A, Walsh A, Williams D (2020) The solar orbiter mission. Science overview. Astron Astrophys 642:A1. https://doi.org/10.1051/0004-6361/202038467. arXiv:2009.00861 [astro-ph.SR]

Nicholson SB (1944) A tornado prominence, June 19, 1944. Publ Astron Soc Pac 56:162. https://doi.org/10.1086/125642

Ofman L, Knizhnik K, Kucera T, Schmieder B (2015) Nonlinear MHD waves in a prominence foot. Astrophys J 813:124. https://doi.org/10.1088/0004-637X/813/2/124. arXiv:1509.07911 [astro-ph.SR]

Öhman Y (1969) Observations of rotational motion in prominences. Sol Phys 9:427–431. https://doi.org/10.1007/BF02391666

Okamoto TJ, Tsuneta S, Berger TE, Ichimoto K, Katsukawa Y, Lites BW, Nagata S, Shibata K, Shimizu T, Shine RA, Suematsu Y, Tarbell TD, Title AM (2007) Coronal transverse magnetohydrodynamic waves in a solar prominence. Science 318:1577. https://doi.org/10.1126/science.1145447. arXiv:0801.1958

Okamoto TJ, Antolin P, De Pontieu B, Uitenbroek H, Van Doorsselaere T, Yokoyama T (2015) Resonant absorption of transverse oscillations and associated heating in a solar prominence. I. Observational aspects. Astrophys J 809:71. https://doi.org/10.1088/0004-637X/809/1/71. arXiv:1506.08965 [astro-ph.SR]

Okamoto TJ, Liu W, Tsuneta S (2016) Helical motions of fine-structure prominence threads observed by hinode and IRIS. Astrophys J 831(2):126. https://doi.org/10.3847/0004-637X/831/2/126. arXiv:1608.00123 [astro-ph.SR]

Orozco Suárez D, Ramos AA, Trujillo Bueno J (2012) Evidence for rotational motions in the feet of a quiescent solar prominence. Astrophys J Lett 761:L25. https://doi.org/10.1088/2041-8205/761/2/L25. arXiv:1211.6980 [astro-ph.SR]

Panasenco O, Martin SF, Velli M (2014) Apparent solar tornado-like prominences. Sol Phys 289:603–622. https://doi.org/10.1007/s11207-013-0337-1. arXiv:1307.2303 [astro-ph.SR]

Panesar NK, Innes DE, Tiwari SK, Low BC (2013) A solar tornado triggered by flares? A + A, vol 549 p A105. https://doi.org/10.1051/0004-6361/201220503

Parenti S (2014) Solar Prominences: Observations. Living Reviews in Solar Physics

Pesnell WD, Thompson BJ, Chamberlin PC (2012) The Solar Dynamics Observatory (SDO). Sol Phys 275(1–2):3–15. https://doi.org/10.1007/s11207-011-9841-3

Pettit E (1919) The great eruptive prominences of May 29 and July 15, 1919. Astrophys J 50:206. https://doi.org/10.1086/142496

Pettit E (1925) The forms and motions of the solar prominences. Publications of the Yerkes Observatory 3:4.iii-XXXVII.1

Pettit E (1932) Characteristic features of solar prominences. Astrophys J 76:9. https://doi.org/10.1086/143396

Pettit E (1941) The rotation of a tornado prominence. Publ Astron Soc Pac 53:289. https://doi.org/10.1086/125348

Pettit E (1943) The properties of solar prominences as related to type. In: Contributions from the Mount Wilson Observatory/Carnegie Institution of Washington, vol 679, pp 1–14

Pettit E (1946) Rotation of tornado prominences determined by dopler effect. Publ Astron Soc Pac 58:150. https://doi.org/10.1086/125796

Pettit E (1950) The evidence for tornado prominences. Publ Astron Soc Pac 62:144. https://doi.org/10.1086/126261

Pike CD, Mason HE (1998) Rotating transition region features observed with the SOHO coronal diagnostic spectrometer. Sol Phys 182:333–348. https://doi.org/10.1023/A:1005065704108

Richardson RS (1940) A tornado prominence of record height. Publ Astron Soc Pac 52:326. https://doi.org/10.1086/125211

Rochus P, Auchère F, Berghmans D, Harra L, Schmutz W, Schühle U, Addison P, Appourchaux T, Aznar Cuadrado R, Baker D, Barbay J, Bates D, BenMoussa A, Bergmann M, Beurthe C, Borgo B, Bonte K, Bouzit M, Bradley L, Büchel V, Buchlin E, Büchner J, Cabé F, Cadiergues L, Chaigneau M, Chares B, Choque Cortez C, Coker P, Condamin M, Coumar S, Curdt W, Cutler J, Davies D, Davison G, Defise JM, Del Zanna G, Delmotte F, Delouille V, Dolla L, Dumesnil C, Dürig F, Enge R, François S, Fourmond JJ, Gillis JM, Giordanengo B, Gissot S, Green LM, Guerreiro N, Guilbaud A, Gyo M, Haberreiter M,

Hafiz A, Hailey M, Halain JP, Hansotte J, Hecquet C, Heerlein K, Hellin ML, Hemsley S, Hermans A, Hervier V, Hochedez JF, Houbrechts Y, Ihsan K, Jacques L, Jérôme A, Jones J, Kahle M, Kennedy T, Klaproth M, Kolleck M, Koller S, Kotsialos E, Kraaikamp E, Langer P, Lawrenson A, Le Clech' JC, Lenaerts C, Liebecq S, Linder D, Long DM, Mampaey B, Markiewicz-Innes D, Marquet B, Marsch E, Matthews S, Mazy E, Mazzoli A, Meining S, Meltchakov E, Mercier R, Meyer S, Monecke M, Monfort F, Morinaud G, Moron F, Mountney L, Müller R, Nicula B, Parenti S, Peter H, Pfiffner D, Philippon A, Phillips I, Plesseria JY, Pylyser E, Rabecki F, Ravet-Krill MF, Rebellato J, Renotte E, Rodriguez L, Roose S, Rosin J, Rossi L, Roth P, Rouesnel F, Roulliay M, Rousseau A, Ruane K, Scanlan J, Schlatter P, Seaton DB, Silliman K, Smit S, Smith PJ, Solanki SK, Spescha M, Spencer A, Stegen K, Stockman Y, Szwec N, Tamiatto C, Tandy J, Teriaca L, Theobald C, Tychon I, van Driel-Gesztelyi L, Verbeeck C, Vial JC, Werner S, West MJ, Westwood D, Wiegelmann T, Willis G, Winter B, Zerr A, Zhang X, Zhukov AN (2020) The solar orbiter EUI instrument: the extreme ultraviolet imager. Astron Astrophys 642:A8. https://doi.org/10.1051/0004-6361/201936663

Rompolt B (1975) Spectral features to be expected from rotational and expansional motions in fine solar structures. Sol Phys 41(2):329–348. https://doi.org/10.1007/BF00154070

Ruan G, Schmieder B, Mein P, Mein N, Labrosse N, Gunár S, Chen Y (2018) On the dynamic nature of a quiescent prominence observed by IRIS and MSDP spectrographs. Astrophys J 865:123. https://doi.org/10.3847/1538-4357/aada08

Scharmer GB, Bjelksjo K, Korhonen TK, Lindberg B, Petterson B (2003) The 1-meter Swedish solar telescope. In: Keil SL, Avakyan SV (eds) Innovative telescopes and instrumentation for solar astrophysics. Society of photo-optical instrumentation engineers (SPIE) conference series, vol 4853, pp 341–350

Scherrer PH, Schou J, Bush RI, Kosovichev AG, Bogart RS, Hoeksema JT, Liu Y, Duvall TL, Zhao J, Title AM, Schrijver CJ, Tarbell TD, Tomczyk S (2012) The Helioseismic and Magnetic Imager (HMI) Investigation for the Solar Dynamics Observatory (SDO). Sol Phys 275(1–2):207–227. https://doi.org/10.1007/s11207-011-9834-2

Schmahl EJ, Orrall FQ (1979) Evidence for continuum absorption above the quiet sun transition region. Astrophys J Lett 231:L41–L44. https://doi.org/10.1086/183001

Schmieder B, Raadu MA, Wiik JE (1991) Fine structure of solar filaments. II - Dynamics of threads and footpoints. Astron Astrophys 252:353–365

Schmieder B, Lin Y, Heinzel P, Schwartz P (2004) Multi-wavelength study of a high-latitude EUV filament. Sol Phys 221(2):297–323. https://doi.org/10.1023/B:SOLA.0000035059.50427.68

Schmieder B, Chandra R, Berlicki A, Mein P (2010) Velocity vectors of a quiescent prominence observed by Hinode/SOT and the MSDP (Meudon). Astron Astrophys 514:A68. https://doi.org/10.1051/0004-6361/200913477. arXiv:0911.5091 [astro-ph.SR]

Schmieder B, Kucera TA, Knizhnik K, Luna M, Lopez-Ariste A, Toot D (2013) Propagating waves transverse to the magnetic field in a solar prominence. Astrophys J 777:108. https://doi.org/10.1088/0004-637X/777/2/108. arXiv:1309.1568 [astro-ph.SR]

Schmieder B, Malherbe JM, Wu ST (eds) (2014) Nature of prominences and their role in space weather, 2014, January. IAU symposium, vol 300

Schmieder B, Tian H, Kucera T, López Ariste A, Mein N, Mein P, Dalmasse K, Golub L (2014) Open questions on prominences from coordinated observations by IRIS, Hinode, SDO/AIA, THEMIS, and the Meudon/MSDP. Astron Astrophys 569:A85. https://doi.org/10.1051/0004-6361/201423922. arXiv:1407.3171 [astro-ph.SR]

Schmieder B, Mein P, Mein N, Levens PJ, Labrosse N, Ofman L (2017) Hα Doppler shifts in a tornado in the solar corona. Astron Astrophys 597:A109. https://doi.org/10.1051/0004-6361/201628771. arXiv:1612.02232 [astro-ph.SR]

Schmieder B, Zapiór M, López Ariste A, Levens P, Labrosse N, Gravet R (2017) Reconstruction of a helical prominence in 3D from IRIS spectra and images. Astron Astrophys 606:A30. https://doi.org/10.1051/0004-6361/201730839. arXiv:1706.08078 [astro-ph.SR]

Secchi PA (1877) Le Soleil, vol 2

Silva SSA, Fedun V, Verth G, Rempel EL, Shelyag S (2020) Solar vortex tubes: vortex dynamics in the solar atmosphere. Astrophys J 898(2):137. https://doi.org/10.3847/1538-4357/ab99a9. arXiv:2007.04371 [astro-ph.SR]

Silva SSA, Verth G, Rempel EL, Shelyag S, Schiavo LACA, Fedun V (2021) Solar vortex tubes. II. On the origin of magnetic vortices. Astrophys J 915(1):24. https://doi.org/10.3847/1538-4357/abfec2

Su Y, Wang T, Veronig A, Temmer M, Gan W (2012) Solar magnetized "tornadoes:" relation to filaments. Astrophys J Lett 756:L41. https://doi.org/10.1088/2041-8205/756/2/L41. arXiv:1208.0138 [astro-ph.SR]

Su Y, Gömöry P, Veronig A, Temmer M, Wang T, Vanninathan K, Gan W, Li Y (2014) Solar magnetized tornadoes: rotational motion in a tornado-like prominence. Astrophys J Lett 785:L2. https://doi.org/10.1088/2041-8205/785/1/L2. arXiv:1312.5226 [astro-ph.SR]

Suematsu Y, Tsuneta S, Ichimoto K, Shimizu T, Otsubo M, Katsukawa Y, Nakagiri M, Noguchi M, Tamura T, Kato Y, Hara H, Kubo M, Mikami I, Saito H, Matsushita T, Kawaguchi N, Nakaoji T, Nagae K, Shimada S, Takeyama N, Yamamuro T (2008) The solar optical telescope of Solar-B (hinode): the optical telescope assembly. Sol Phys 249:197–220. https://doi.org/10.1007/s11207-008-9129-4

Tei A, Gunár S, Heinzel P, Okamoto TJ, Štěpán J, Jejčič S, Shibata K (2020) IRIS Mg II observations and non-LTE modeling of off-limb spicules in a solar polar coronal hole. Astrophys J 888(1):42. https://doi.org/10.3847/1538-4357/ab5db1. arXiv:1911.12243 [astro-ph.SR]

Tripathi D, Isobe H, Jain R (2009) Large amplitude oscillations in prominences. Space Sci Rev 149:283–298. https://doi.org/10.1007/s11214-009-9583-9. arXiv:0910.4059 [astro-ph.SR]

Tsuneta S, Ichimoto K, Katsukawa Y, Nagata S, Otsubo M, Shimizu T, Suematsu Y, Nakagiri M, Noguchi M, Tarbell T, Title A, Shine R, Rosenberg W, Hoffmann C, Jurcevich B, Kushner G, Levay M, Lites B, Elmore D, Matsushita T, Kawaguchi N, Saito H, Mikami I, Hill LD, Owens JK (2008) The solar optical telescope for the hinode mission: an overview. Sol Phys 249:167–196. https://doi.org/10.1007/s11207-008-9174-z. arXiv:0711.1715

Tziotziou K, Tsiropoula G, Kontogiannis I, Scullion E, Doyle JG (2018) A persistent quiet-sun small-scale tornado. I. Characteristics and dynamics. Astron Astrophys 618:A51. https://doi.org/10.1051/0004-6361/201833101

Tziotziou K, Scullion E, Shelyag S, Steiner O, Khomenko E, Tsiropoula G, Canivete Cuissa JR, Wedemeyer S, Kontogiannis I, Yadav N, Kitiashvili IN, Skirvin SJ, Dakanalis I, Kosovichev AG, Fedun V (2023) Vortex motions in the solar atmosphere. Space Sci Rev 219(1):1. https://doi.org/10.1007/s11214-022-00946-8

Vial JC, Engvold O (eds) (2015) Solar prominences. Astrophysics and space science library, vol 415

Wang W, Liu R, Wang Y (2017) January. Tornado-like evolution of a kink-unstable solar prominence. Astrophys J 834(1):38. https://doi.org/10.3847/1538-4357/834/1/38. arXiv:1611.04667 [astro-ph.SR]

Warren HP, Brooks DH, Ugarte-Urra I, Reep JW, Crump NA, Doschek GA (2018) Spectroscopic observations of current sheet formation and evolution. Astrophys J 854:122. https://doi.org/10.3847/1538-4357/aaa9b8. arXiv:1711.10826 [astro-ph.SR]

Wedemeyer S, Steiner O (2014) On the plasma flow inside magnetic tornadoes on the Sun. Publ Astron Soc Jpn 66:S10. https://doi.org/10.1093/pasj/psu086. arXiv:1406.7270 [astro-ph.SR]

Wedemeyer S, Scullion E, Rouppe van der Voort L, Bosnjak A, Antolin P (2013) Are giant tornadoes the legs of solar prominences? Astrophys J 774:123

Wedemeyer S, Scullion E, Steiner O, de la Cruz Rodriguez J, Rouppe van der Voort LHM (2013) Magnetic tornadoes and chromospheric swirls - definition and classification. J Phys Conf Ser 440(1):012005. https://doi.org/10.1088/1742-6596/440/1/012005. arXiv:1303.0179 [astro-ph.SR]

Wedemeyer-Böhm S, Scullion E, Steiner O, Rouppe van der Voort L, de La Cruz Rodriguez J, Fedun V, Erdélyi R (2012) Magnetic tornadoes as energy channels into the solar corona. Nature 486:505–508. https://doi.org/10.1038/nature11202

Yadav N, Cameron RH, Solanki SK (2020) Simulations show that vortex flows could heat the chromosphere in solar plage. Astrophys J Lett 894(2):L17. https://doi.org/10.3847/2041-8213/ab8dc5. arXiv:2004.13996 [astro-ph.SR]

Yadav N, Cameron RH, Solanki SK (2021) Vortex flow properties in simulations of solar plage region: evidence for their role in chromospheric heating. Astron Astrophys 645:A3. https://doi.org/10.1051/0004-6361/202038965. arXiv:2010.14971 [astro-ph.SR]

Yang Z, Tian H, Peter H, Su Y, Samanta T, Zhang J, Chen Y (2018) Two solar tornadoes observed with the interface region imaging spectrograph. Astrophys J 852:79. https://doi.org/10.3847/1538-4357/aa9e04. arXiv:1711.08968 [astro-ph.SR]

Young PR, O'Dwyer B, Mason HE (2012) Velocity measurements for a solar active region fan loop from Hinode/EIS Observations. Astrophys J 744:14. https://doi.org/10.1088/0004-637X/744/1/14. arXiv:1107.2362 [astro-ph.SR]

Zapiór M, Martínez-Gómez D (2016) Direct detection of the helical magnetic field geometry from 3D reconstruction of prominence knot trajectories. Astrophys J 817:123. https://doi.org/10.3847/0004-637X/817/2/123

Zapiór M, Rudawy P (2012) Estimation of solar prominence magnetic fields based on the reconstructed 3D trajectories of prominence knots. Sol Phys 280:445–456. https://doi.org/10.1007/s11207-012-0072-z. arXiv:1207.2005 [astro-ph.SR]

Zapiór M, Kotrč P, Rudawy P, Oliver R (2015) Simultaneous observations of solar prominence oscillations using two remote telescopes. Sol Phys 290:1647–1659. https://doi.org/10.1007/s11207-015-0696-x

Zhang QM, Chen PF, Xia C, Keppens R, Ji HS (2013) Parametric survey of longitudinal prominence oscillation simulations. Astron Astrophys 554:124

Zhong S, Li K (1994) Observation and study of the tornado-like prominence on August 29, 1990. In: Publications of the Yunnan observatory, vol 4, pp 1–6

Zhou YH, Xia C, Keppens R, Fang C, Chen PF (2018) Three-dimensional MHD simulations of solar prominence oscillations in a magnetic flux rope. Astrophys J 856(2):179
Zirker JB, Engvold O, Martin SF (1998) Counter-streaming gas flows in solar prominences as evidence for vertical magnetic fields. Nature 396(6710):440–441. https://doi.org/10.1038/24798

Authors and Affiliations

Stanislav Gunár[1] · Nicolas Labrosse[2] · Manuel Luna[3] · Brigitte Schmieder[4,5,2] · Petr Heinzel[1,6] · Therese A. Kucera[7] · Peter J. Levens[2] · Arturo López Ariste[8] · Duncan H. Mackay[9] · Maciej Zapiór[1]

✉ S. Gunár
gunar@asu.cas.cz

1 Astronomical Institute, The Czech Academy of Sciences, 251 65 Ondřejov, Czech Republic

2 SUPA, School of Physics & Astronomy, University of Glasgow, Glasgow, United Kingdom

3 Departament de Física, Universitat de les Illes Balears, E-07122 Palma de Mallorca, Spain

4 LESIA, Observatoire de Paris, Université PSL, CNRS, Sorbonne Université, Université de Paris, 5 place Janssen, 92290 Meudon Principal Cedex, France

5 Centre for mathematical Plasma Astrophysics, Dept. of Mathematics, KU Leuven, 3001 Leuven, Belgium

6 Centre of Scientific Excellence — Solar and Stellar Activity, University of Wroclaw, Wroclaw, Poland

7 Heliophysics Science Division, NASA Goddard Space Flight Center, Greenbelt, MD 20771, USA

8 IRAP, Université de Toulouse, CNRS, CNES, UPS. 14, Av. E. Belin, 31400 Toulouse, France

9 School of Mathematics and Statistics, University of St Andrews, North Haugh, St Andrews, Fife KY16 9SS, UK